

Zhu *et al.* (2022) Barley *ELF3* alleles tune phenotypic plasticity in response to high temperature

RESEARCH PAPER

## **An exotic allele of barley *EARLY FLOWERING 3* contributes to developmental plasticity at elevated temperatures**

5

Zihao Zhu<sup>1</sup>, Finn Esche<sup>1</sup>, Steve Babben<sup>1</sup>, Jana Trenner<sup>1</sup>, Albrecht Serfling<sup>2</sup>, Klaus Pillen<sup>3</sup>, Andreas Maurer<sup>3</sup>, and Marcel Quint<sup>1,4\*</sup>

10 <sup>1</sup> Institute of Agricultural and Nutritional Sciences, Martin Luther University Halle-Wittenberg, Betty-Heimann-Str. 5, D-06120, Halle (Saale), Germany

<sup>2</sup> Institute for Resistance Research and Stress Tolerance, Julius Kuehn-Institute, Erwin-Baur-Str. 27, D-06484, Quedlinburg, Germany

<sup>3</sup> Chair of Plant Breeding, Institute of Agricultural and Nutritional Sciences, Martin Luther University Halle-Wittenberg, Betty-Heimann-Str. 3, D-06120, Halle (Saale), Germany

15 <sup>4</sup> German Centre for Integrative Biodiversity Research, Halle-Jena-Leipzig, Puschstrasse 4, D-04103, Leipzig, Germany

\* [marcel.quint@landw.uni-halle.de](mailto:marcel.quint@landw.uni-halle.de)

20

### **Highlight**

We demonstrate that an exotic allele of *EARLY FLOWERING 3* (*ELF3*) contributes to plant architectural and developmental acclimation, and thereby improves yield stability at high ambient temperatures.

25

30

35

Zhu *et al.* (2022) Barley *ELF3* alleles tune phenotypic plasticity in response to high temperature

## 40 Abstract

Increase in ambient temperatures caused by climate change affects various morphological and developmental traits of plants, threatening crop yield stability. In the model plant *Arabidopsis thaliana*, *EARLY FLOWERING 3* (*ELF3*) plays prominent roles in temperature sensing and thermomorphogenesis signal transduction. However, how crop species respond to elevated temperatures is  
45 poorly understood. Here, we show that the barley ortholog of *AtELF3* interacts with high temperature to control growth and development. We used heterogeneous inbred family (HIF) pairs generated from a segregating mapping population and systematically studied the role of exotic *ELF3* variants in barley temperature responses. An exotic *ELF3* allele from Syrian origin promoted elongation growth in barley at elevated temperatures, whereas plant area and estimated biomass were  
50 drastically reduced, resulting in an open canopy architecture. The same allele accelerated inflorescence development at high temperature, which correlated with early transcriptional induction of MADS-box floral identity genes *BM3* and *BM8*. Consequently, barley plants carrying the exotic *ELF3* allele displayed stable total grain number and mitigated yield loss at elevated temperatures. Our findings therefore demonstrate that exotic *ELF3* variants can contribute to phenotypic and developmental acclimation to elevated temperatures, providing a stimulus for breeding of climate resilient crops.  
55

**Keywords:** barley, climate change, development, *EARLY FLOWERING 3*, heterogeneous inbred family, plant acclimation, plant architecture, thermomorphogenesis, yield stability  
60

## Introduction

Climate change has unequivocally disrupted human and natural systems. With the global temperature predicted to reach a 1.5°C increase in the near term, global warming poses significant challenges to ecosystems and food security. The agricultural responses to global warming are of great concerns, as elevated ambient temperatures limit the productivity and spatial distribution of crop plants, resulting in severe yield losses (Leng and Huang, 2017; Zhao *et al.*, 2017). Understanding how plants respond to elevated temperatures is pivotal to achieve crop-level adaptations and yield  
70 stability in the context of global climate change (Challinor *et al.*, 2014; Chen *et al.*, 2022).

Plants are constantly exposed to changing environments and are capable to adapt their growth and development accordingly. Morphological and developmental adjustments of plants induced by elevated ambient temperatures are collectively termed thermomorphogenesis (Quint *et al.*, 2016).  
75 Our understanding of molecular genetic processes underlying thermomorphogenesis is mainly

Zhu *et al.* (2022) Barley *ELF3* alleles tune phenotypic plasticity in response to high temperature

based on studies in the model plant *Arabidopsis thaliana*. In *Arabidopsis*, changes in ambient temperature are perceived via multiple systems. The photoreceptor phytochrome B (phyB) was the first identified plant temperature sensor, integrating light and temperature sensing (Jung *et al.*, 2016; Legris *et al.*, 2016). Warm temperatures accelerate the thermal/dark reversion of phyB from its active to its inactive form, thereby relieving the repression of the basic helix-loop-helix (bHLH) transcription factor PHYTOCHROME INTERACTING FACTOR 4 (PIF4) (reviewed in Delker *et al.*, 2017). As a central regulatory hub of thermomorphogenesis signalling, PIF4 activates auxin biosynthesis genes, mediating elongation growth and leaf hyponasty at warm temperatures to improve the transpirational cooling capacity (Koini *et al.*, 2009; Franklin *et al.*, 2011; Crawford *et al.*, 2012; Park *et al.*, 2019). On the other hand, PIF4 mediates thermal acceleration of flowering by activating *FLOWERING LOCUS T (FT)* (Kumar *et al.*, 2012). In addition to the phyB-PIF4-auxin signalling module, recent studies revealed prominent roles of the circadian clock component EARLY FLOWERING 3 (*ELF3*) in the *Arabidopsis* thermomorphogenic pathway (Box *et al.*, 2015; Raschke *et al.*, 2015). As an integral part of the plant circadian oscillator, the scaffold protein *ELF3* interacts with LUX ARRHYTHMO (*LUX*) and *ELF4* to form the evening complex (EC) (Nusinow *et al.*, 2011; Herrero *et al.*, 2012). The EC directly represses the transcription of circadian clock components, as well as clock output genes such as *PIF4* (Huang and Nusinow, 2016). The prion-like domain of *ELF3* functions as a thermosensor and enables the phase separation of *ELF3* into liquid droplets at high temperatures, relieving the transcriptional repression of *PIF4* and potentially the direct interaction with PIF4 (Ezer *et al.*, 2017; Jung *et al.*, 2020). Consequently, *ELF3* integrates temperature signals to the circadian oscillator, controlling rhythmic thermoresponsive outputs (Zhu *et al.*, 2022). However, although *ELF3* homologs have been identified in a wide range of crop species (Faure *et al.*, 2012; Zakhrebekova *et al.*, 2012; Ning *et al.*, 2015; Alvarez *et al.*, 2016; Lu *et al.*, 2017; Ridge *et al.*, 2017), signalling components and regulation of thermomorphogenesis are largely unknown in non-model species.

As a globally cultivated crop, barley (*Hordeum vulgare* L.) has emerged as an excellent model for understanding crop adaptation to elevated temperatures (Dawson *et al.*, 2015). The current understanding of barley temperature responses is mainly restricted to the temperature effects on reproductive development. The barley ortholog of *AtELF3* (also known as *EARLY MATURITY 8* or *Praematurum-a*) controls flowering time, and plays a critical role in barley adaptation to short growing seasons (Faure *et al.*, 2012; Zakhrebekova *et al.*, 2012). In barley, loss of *ELF3* function facilitates the expression of the photoperiod response gene *PHOTOPERIOD H1 (Ppd-H1)*, which corresponds to *Arabidopsis* circadian clock gene *PSEUDO RESPONSE REGULATOR 37 (PRR37)* (Turner *et al.*, 2005; Faure *et al.*, 2012). Up-regulation of *Ppd-H1* promotes the expression of *FT1*, a barley homolog of *Arabidopsis FT* (Campoli *et al.*, 2012). Induction of *FT1* is associated with the expression of barley floral meristem identity genes *VERNALIZATION 1 (VRN1)*, *BARLEY MADS-*

Zhu *et al.* (2022) Barley *ELF3* alleles tune phenotypic plasticity in response to high temperature

115 *box 3 (BM3)*, and *BM8*, promoting inflorescence development (Trevaskis *et al.*, 2007; Li *et al.*, 2015). Alternatively, the loss of *ELF3* function mediates gibberellin (GA) biosynthesis, which cooperates with *FT1* in the acceleration of flowering (Boden *et al.*, 2014).

120 Under high ambient temperatures, the floral development of barley is accelerated in an *ELF3* loss-of-function background, even with reduced or invariable *FT1* transcript levels, suggesting the involvement of *FT1*-independent pathways (Hemming *et al.*, 2012; Ejaz and von Korff, 2017). For example, as a core component in the barley circadian network, *ELF3* controls the thermo-responsiveness of *GIGANTEA (GI)* and *PRR* genes (Ford *et al.*, 2016; Müller *et al.*, 2020). Moreover, acting downstream of *ELF3*, the effects of *Ppd-H1* in thermoresponsive flowering depend on the allelic variation for *VRN1*, indicating the interaction with vernalization pathways (Ejaz and von Korff, 2017; Ochagavía *et al.*, 2021). These findings suggest critical upstream roles of *ELF3* function in the genetic control of barley developmental responses to elevated temperatures.

125 In addition to induced loss of function mutants, exploiting natural variation provides another approach to improve crop adaptation. Barley germplasm consists of genetically diverse landraces and exotic accessions, a large proportion of which is presumed to be adapted to various abiotic stresses (Newton *et al.*, 2011; Russell *et al.*, 2011). In the context of *ELF3*, for instance, a spontaneous recessive *elf3* mutant was identified in barley landraces from the Qinghai-Tibetan Plateau, where the growing season is restricted by low temperatures (Xia *et al.*, 2017). To investigate the potential value of exotic barley accessions, the nested association mapping (NAM) population Halle Exotic Barley-25 (HEB-25) was generated by crossing 25 wild barley accessions with the elite cultivar Barke (Maurer *et al.*, 2015). Aiming to study the effects of exotic *ELF3* variants, heterogeneous inbred family (HIF) pairs were generated based on HEB-25 (Zahn *et al.*, 2022, Preprint). In each HIF pair, two nearly isogenic sister lines differ only in the homozygous cultivated (elite) or exotic (wild) *ELF3* allele, allowing direct comparison. Our recent findings from field experiments revealed significant roles of exotic *ELF3* alleles in barley development and grain yield, validating the previous quantitative trait locus (QTL) analysis (Maurer *et al.*, 2016; Zahn *et al.*, 2022, Preprint).

145 In this study, we systematically investigate the role of exotic *ELF3* alleles in barley temperature responses during seedling establishment, vegetative growth, and reproductive development. We demonstrate that at least one exotic *ELF3* allele interacts with elevated temperatures to modulate growth, development, and grain yield of barley.

5 Zhu *et al.* (2022) Barley *ELF3* alleles tune phenotypic plasticity in response to high temperature

## 150 **Materials and methods**

### **Plant Materials and growth conditions**

We selected three HIF pairs (10\_190, 16\_105 and 17\_041) generated from the two-rowed spring barley NAM population HEB-25, with exotic barley accessions collected from Syria, Afghanistan, and Iran, respectively (Maurer *et al.*, 2015; Zahn *et al.*, 2022, Preprint). The genomic setup of these three HIF pairs were previously described and is visualized in Supplementary Fig. S1 (Anand and Rodriguez Lopez, 2022; Zahn *et al.*, 2022, Preprint). Bowman and *elf3*<sup>BW290</sup> (*elf3/eam8.w* loss-of-function mutant BW290 in Bowman background) were used as controls.

For the growth and development experiment, seeds were directly sown in soil and placed in growth chambers with day/night temperatures of 20°C/16°C, light intensity of 300  $\mu\text{mol m}^{-2}\text{s}^{-1}$  and long day photoperiod (LD; 16 h light/8 h dark). Five days after sowing (DAS), uniformly germinated seedlings were selected, and then either shifted to high ambient day/night temperatures (28°C/24°C, hereafter called 28°C treatment) or were kept at the 20°C/16°C temperature regime (hereafter called 20°C treatment). The position of plants in the phytochambers was randomly rotated twice per week. Eleven plants equaling eleven biological replicates from each genotype were used in each temperature condition.

The yield experiment was conducted at Julius Kühn-Institut (Quedlinburg, Germany). Seeds of the mutant *elf3*<sup>BW290</sup>, its corresponding cultivar Bowman, and HIF pair 10\_190 (hereafter called HIF pair 10) seeds were coated with Rubin TT (BASF, Ludwigshafen, Germany) to avoid fungal infections before being sown in soil. Plants were grown in a greenhouse under the 20°C treatment, light intensity of 300  $\mu\text{mol m}^{-2}\text{s}^{-1}$  and LD (16 h light/8 h dark). Plants that reached BBCH-13 (Lancashire *et al.*, 1991) were either shifted to the 28°C treatment conditions or were kept under the 20°C treatment. Twelve to fifteen plants from each genotype were used in each temperature condition.

175

### **Temperature assay on plates**

Bowman and *elf3*<sup>BW290</sup> seeds were sterilized with 4% NaClO for 30 min and were cold stratified at 4°C for 2 d in darkness. Seeds were sown on solid *Arabidopsis thaliana* solution (ATS) nutrient medium with 1% (w/v) sucrose (Lincoln *et al.*, 1990). Vertically oriented plates were placed in darkness at 20°C to allow germination. After germination, seedlings were shifted to constant 28°C or were kept at constant 20°C, with LD (16 h light/8 h dark) and light intensity of 90  $\mu\text{mol m}^{-2}\text{s}^{-1}$ . Leaf tips were marked after germination and seedlings were imaged in two consecutive days at Zeitgeber time (ZT) 08. The leaf length (from the marked position) was measured using RootDetection 0.1.2 (<http://www.labutils.de/rd.html>). Nine to seventeen seedlings from each genotype were used in each temperature condition.

185

Zhu *et al.* (2022) Barley *ELF3* alleles tune phenotypic plasticity in response to high temperature

## Construction of image-based phenotyping platform

To non-destructively acquire plant growth phenotypes, we constructed an image-based phenotyping platform. We customized a 1.2 m × 1.2 m × 1.8 m phenotyping frame with a stand positioned in the middle of the frame to fix the position and direction of the plants during each imaging time point. The platform included three Raspberry Pi 3 model B single-board microcomputers and three Raspberry Pi RGB camera modules (V2 8MP, Raspberry Pi foundation, Cambridge, England, UK), which enabled imaging from three directions: two side-views separated by 90° and a top-view. The lighting was provided by two light-emitting diodes (LED) lamps (4.6W, Philips, Eindhoven, Netherlands) from the top, and two LED light sets (10W, Neewer, Shenzhen, China) from the sides. The camera modules and light sets were positioned on the top of the frame or outside of it using tripods. The lens-pot distances were 1.25 m to the middle of the pot for side-views and 1.3 m to the top of the pot surface for top-view. To distinguish the plant parts from the surroundings, white foils (Colormatt-Hintergrund Super White, Studioexpress Vertriebs GmbH, Wiernsheim, Germany) were used as imaging background, blue cages (HNP Metalltechnik GmbH, Quedlinburg, Germany) were added to all pots, and blue meshes (Klartext Wunderlich Coating GmbH & Co. KG, Osterode am Harz, Germany) were used to cover the soil surface from 8 DAS.

The Raspberry Pi operation protocol for simultaneously acquiring plant images from several angles was previously described (Tovar *et al.*, 2018). To use Windows computer as a remote host for Raspberry Pi, we used secure copy protocol (scp) to copy the public secure shell (SSH) key, and the rsync package was installed using Cygwin (<https://www.cygwin.com>) for proper synchronization of images.

## Phenotyping

For the growth and development experiment, plant height was manually measured without straightening the plants on a daily basis between 5 DAS and 14 DAS. From 8 DAS until 52 DAS, besides the manual measurement of plant height, total tiller number was counted, and each plant was imaged every two to four days. The images were analyzed with the HTPHeno pipeline (Hartmann *et al.*, 2011) for plant height (two side-views) and plant area (all three views). The plant volume was calculated as the square root of the product of two side-view areas and the top-view area. For convex hull area, the plant silhouette images derived from the HTPHeno pipeline were further analyzed using the Hull and Circle plugin (Karperien, A., version 2.0a) in ImageJ (<http://image.nih.gov/ij/>). The days until visible third leaf, coleoptile tiller, first tiller, flag leaf sheath opening, and heading (first visible awns) were scored on a daily basis. The chlorophyll content was measured using the SPAD-502Plus chlorophyll meter (Konica Minolta, Chiyoda City, Tokyo, Japan) every week from 16 DAS until 52 DAS. The measurement took place at the same position: around 3 cm from the



Zhu *et al.* (2022) Barley *ELF3* alleles tune phenotypic plasticity in response to high temperature

leaf collar of the second leaf. For destructive measurement of leaf size, plants ( $n=5$ ) were harvested and the first and second leaves were imaged 16 DAS. The leaf length and width of the first and second leaves were measured using ImageJ (<http://image.nih.gov/ij/>). The measurement of leaf width took place at 2 cm from the leaf collar. All measurements and imaging were conducted between ZT03 and ZT06 on each measurement day.

For the yield experiment, the developmental stage was scored at 73 DAS. Plant height and total tiller number were scored at 118 DAS. At maturity (166 DAS for 28°C and 195 DAS for 20°C), the arial part of the plants was harvested. From three randomly selected spikes of each plant, the number of grains and florets per spike was determined, and the length of the spike (excluding the awns) was measured. The averaged data of each plant were used for further analysis. Plant dry weight was measured after placing plant material (arial parts excluding the spikes) into a drying oven for 1 d at 60°C. The grains were threshed using the LD180 laboratory thresher (Wintersteiger, Ried im Innkreis, Austria). The number of grains per plant, grain area, thousand grain weight, and grain yield per plant were measured using MARViN ProLine seed analyzer (MARVITECH GmbH, Wittenburg, Germany).

#### 240 **Analysis of transcript levels**

Plants from HIF pair 10\_190 (10\_elite and 10\_wild) were grown under conditions as described above for the growth and development experiment. The temperature treatments started at 5 DAS. Leaf samples were harvested at ZT08 at 5, 12, 19, 27, 33, and 40 DAS, with three biological replicates each.

Total RNA was extracted using the NucleoSpin RNA Plant Kit (Macherey-Nagel), cDNA was synthesized using the PrimeScript RT Reagent Kit (Perfect Real Time, Takara Bio), and quantitative real-time-PCR was performed on an AriaMx Real-Time PCR System (Agilent) using Absolute Blue Low Rox Mix (Thermo Fisher Scientific). The expression of target genes was normalized to *HvACTIN* and *HvGAPDH* (Kikuchi *et al.*, 2012; Zakhrebekova *et al.*, 2012). Primer sequences are described in Supplementary Table S1.

#### **Analysis of *ELF3* sequence in HIF pairs**

The *ELF3* coding sequences of HIF parental lines were described previously (Zahn *et al.*, 2022, Preprint). In this study, the entire *ELF3* genomic sequence present in three HIF pairs was amplified using Ex Taq DNA Polymerase (Takara Bio, Kusatu, Shiga, Japan) and 1186 bp of promoter sequence upstream of the *ELF3* start codon in HIF pair 10 was amplified using ALLin™ RPH Polymerase (highQu GmbH, Kraichtal, Germany). The amplicons were submitted to Eurofins Genomics (Ebersberg, Germany) for dideoxy sequencing. The PCR and sequencing primers used for ge-

Zhu *et al.* (2022) Barley *ELF3* alleles tune phenotypic plasticity in response to high temperature

260 nomic sequence have been described previously (Zahn *et al.*, 2022, Preprint) and those used for promoter sequence are shown in Supplementary Table S1. The sequences were aligned and compared to their corresponding parental lines (Zahn *et al.*, 2022, Preprint) as well as their corresponding sister line in each HIF pair using MAFFT version 7 (Katoch *et al.*, 2019).

### 265 **Growth curve modeling**

Growth curves were modeled for all traits which were obtained on successive days during growth and development experiment, as cubic splines in SAS PROC TRANSREG (SAS Institute, Inc., Cary, USA) with nknots set 1. Based on the predicted values the following parameters were derived for each line: maximum increase (difference between two consecutive days), day of maximum increase, maximum value, day of maximum value, end point value, and total area under the curve (based on the trapezoidal rule with trapezoids defined between each two consecutive days).

### **Principal component analysis (PCA)**

PCA was performed with SAS PROC PRINCOMP (SAS Institute, Inc., Cary, USA) based on the arithmetic means of all obtained traits from the growth and development experiment, or the derived growth curve modeling traits, for each line. Due to the different units and scales of the traits, the PCA was based on the correlation matrix.

### **Pairwise correlation analysis of traits**

280 Pairwise correlation coefficients were determined for lines Bowman, *elf3*<sup>BW290</sup>, and HIF pair 10 between all investigated traits obtained from both growth and development, and yield experiments. As for PCA, correlations across all lines were based on the arithmetic means, as well as the derived growth curve modeling traits. All Pearson correlation coefficients and their *P* values were computed using SAS PROC CORR (SAS Institute, Inc., Cary, USA).

285

### **Statistical analysis**

Significant differences between temperature treatments and genotypes were analyzed by two-way ANOVA followed by Tukey's HSD post-hoc test in R (R Core Team, 2013). Significant differences between two time points were analyzed by a two-sided Student's *t*-test using GraphPad Quick-Calcs (<http://graphpad.com/quickcalcs/>). Linear regression was calculated and plotted using the `stat_poly_eq` function from the R package `ggpmisc` (Aphalo, 2016).

295



Zhu *et al.* (2022) Barley *ELF3* alleles tune phenotypic plasticity in response to high temperature

## Results

### ***ELF3* is involved in barley thermomorphogenesis**

In the model plant *Arabidopsis thaliana*, elevated temperatures induce a series of morphological and architectural changes, with hypocotyl elongation as a classic phenotype to represent thermo-responsiveness (Quint *et al.*, 2016). The *Arabidopsis elf3* mutants generally display exaggerated hypocotyl growth even at relatively low temperatures, possibly due to lack of thermosensing functions (Box *et al.*, 2015; Raschke *et al.*, 2015; Jung *et al.*, 2020; Zhu *et al.*, 2022). To assess the possible role of *ELF3* in barley thermomorphogenesis, we first performed a temperature assay on agar plates mimicking the standard growth conditions for *Arabidopsis* seedling assays. Leaf length was measured of cultivar Bowman and *elf3*<sup>BW290</sup> mutant seedlings grown in LD at constant 20°C or 28°C. In two consecutive days after germination, we observed no difference in leaf length between Bowman and *elf3*<sup>BW290</sup> at 20°C (Fig. 1). However, at 28°C *elf3*<sup>BW290</sup> displayed longer leaves, compared to Bowman (Fig. 1). This suggests that *ELF3* is involved in the early temperature response of barley seedlings, controlling elongation growth in a negative manner similar to the role of *Arabidopsis ELF3* (Box *et al.*, 2015; Raschke *et al.*, 2015).

To further study the role of *ELF3* in barley temperature response, in addition to Bowman and *elf3*<sup>BW290</sup>, we selected three HIF pairs (10\_190, 16\_105 and 17\_041) from the barley NAM population HEB-25 (Maurer *et al.*, 2015; Maurer *et al.*, 2016), which displayed differences for several developmental phenotypes between the HIF sister lines in previous field experiments (Zahn *et al.*, 2022, Preprint). Each HIF pair contains two near-isogenic lines (NILs), carrying either *HvELF3* (elite) from cultivar Barke or *HspELF3* (wild, *Hsp* = *Hordeum vulgare* L. ssp. *spontaneum*) from exotic barley accessions (Supplementary Fig. S1). In this study, we initially determined the full-length genomic sequence of *ELF3* in the three used HIF pairs and compared them to the previously sequenced parental lines (Zahn *et al.*, 2022, Preprint). We observed a W669G substitution in all three wild lines. Furthermore, the 16\_105\_ *HspELF3* (hereafter called 16\_wild) and 17\_wild HIF pairs belong to the same haplotype carrying four additional non-synonymous single-nucleotide polymorphisms (SNPs) in *ELF3* compared to 10\_wild (Fig. 2). In line with the previous observation using barley landraces collected from the Qinghai-Tibetan Plateau (Xia *et al.*, 2017), we identified SNPs and insertion-deletion mutations (Indels) especially in intron 2 of *ELF3* in 16\_wild and 17\_wild (Fig. 2). However, the previously described alternative splicing mutation in intron 3 was not observed in our HIF lines (Xia *et al.*, 2017). In our previous field experiments, we identified the strongest effects on shooting and heading within HIF pair 10, which could be validated also in controlled environments (Zahn *et al.*, 2022, Preprint). Consistent with the phenotypes, we also observed differences in transcription levels of downstream genes *FT1* and *VRN1*, which are known to be regulated via *ELF3*, between 10\_elite and 10\_wild, without changes in *ELF3* transcript levels (Zahn *et al.*, 2022, Preprint). Structural modeling of *ELF3* protein variants predicted a potential in-

10 Zhu *et al.* (2022) Barley *ELF3* alleles tune phenotypic plasticity in response to high temperature

fluence of the W669G mutation on protein structure, which might be responsible for the observed phenotypic differences (Fig. 2) (Zahn *et al.*, 2022, Preprint). Hence, although the previous field and indoor experiments were not performed in a temperature context, using these phenotypically divergent HIF pairs promised to provide a suitable genetic background to study the role of exotic *ELF3* alleles in barley temperature response. In the following, we systematically analyzed the role of *ELF3* on temperature-sensitive development in general by comparing Bowman and *elf3<sup>BW290</sup>*, and with a specific focus on natural variation between exotic *ELF3* alleles by comparing the sister lines of the three above mentioned HIF lines. We divided development into early seedling establishment, vegetative growth, and reproductive growth.

### Elevated temperatures accelerate barley seedling establishment

To investigate the effect of *ELF3* and elevated temperatures on barley growth and development during early vegetative development, the eight described genotypes were grown in LD with day/night temperatures of 20°C/16°C (20°C treatment) or 28°C/24°C (28°C treatment). The temperature treatments started 5 days after sowing (DAS), and the first phenotype, plant height, was measured on a daily basis until 14 DAS (Fig. 3A; Supplementary table S2). We observed that at elevated temperatures, plant height was significantly increased in *elf3<sup>BW290</sup>* from 6 DAS on. This effect was also present in the corresponding cultivar Bowman, but much delayed (reliably from 13 to 14 DAS on, Fig. 3A; Supplementary table S2). As observed in the temperature assay on plates (Fig. 1), the differences in plant height between Bowman and *elf3<sup>BW290</sup>* were mostly observed at 28°C but not at 20°C (Fig. 1; Fig. 3A; Supplementary table S2). Hence, plant height is obviously a phenotype that is conditionally regulated by barley *ELF3* at elevated temperature during early vegetative growth. Similar results were obtained for HIF pair 10, with 10\_wild showing a stronger temperature response compared to 10\_elite (Fig. 3A; Supplementary table S2), suggesting a genetic effect of the exotic barley allele on plant height during early vegetative development. In contrast, in HIF pairs 16 and 17, only temperature effects could be detected, but no allelic differences between the underlying *ELF3* variants (Fig. 3A; Supplementary table S2). Interestingly, we observed pauses of plant height increase in all genotypes during the establishment of barley seedlings, most likely because plant height was first dominated by the length of the first leaf, before the second leaf took over (Fig. 3A, B; Supplementary table S2). Notably, these pauses in plant height increase occurred earlier at elevated temperatures in almost all genotypes (Fig. 3A; Supplementary table S2), indicating accelerated growth and development.

To test for accelerated development, we scored the formation of the third leaf (L3) and the first tiller (T1) under 20°C or 28°C treatment (Fig. 3B, C). In line with the results shown so far (Fig. 1; Fig. 3A; Supplementary table S2), *elf3<sup>BW290</sup>* displayed earlier third leaf formation compared to Bowman at 28°C but not at 20°C (Fig. 3C). In contrast, the formation of the first tiller in both Bowman and

Zhu *et al.* (2022) Barley *ELF3* alleles tune phenotypic plasticity in response to high temperature

370 *elf3*<sup>BW290</sup> was neither genotype nor temperature dependent (Fig. 3C). Except for the first tiller formation in 10\_elite, elevated temperatures generally accelerated the formation of the third leaf and the first tiller in HIF pairs independent of *ELF3* alleles (Fig. 3C). Prior to first tiller formation, barley seedlings can develop coleoptile tillers (T0), which arise from below ground (Fig. 3B). Coleoptile tiller development was known to be related to seedling vigor in wheat (Liang and Richards, 1994; 375 Fujita *et al.*, 2000), and can be suppressed by high ambient temperatures (Cannell, 1969). In confirmation of these reported observations, coleoptile tillers were largely absent at elevated temperatures, especially in Bowman and HIF pair 10 with no coleoptile tiller on 18 DAS, suggesting less vigorous seedlings despite (or maybe rather because of) accelerated growth and development (Supplementary Fig. S2).

380

In addition to accelerated development, elevated temperatures also cause morphological changes, for example narrower leaves in wheat (reviewed in Lippmann *et al.*, 2019). To test whether leaf shape was influenced by temperature, we measured length and width of the first and the second leaves at 16 DAS under 20°C or 28°C treatment (Fig. 3D; Supplementary Table S3). We observed 385 no difference in length or width in the first leaf of each genotype, possibly due to its initiation before the start of the temperature treatments (Fig. 3D; Supplementary Table S3). However, significantly narrower second leaves were observed at elevated temperatures regardless of the genotype, whereas the leaf length did not differ, suggesting reduced leaf area as previously reported (Fig. 3D; Supplementary Table S3) (Lippmann *et al.*, 2019). Taken together, these results demonstrate 390 that early seedling establishment is accelerated by elevated temperatures in barley, with *ELF3* alleles mainly affecting plant height.

### **An exotic *ELF3* allele affects barley growth and architecture at elevated temperatures**

As we observed significant effects of elevated temperatures on multiple phenotypes during barley 395 seedling establishment (Fig. 3; Supplementary Fig. S2; Supplementary Tables S2, S3), we next asked whether the growth of barley plants would be further affected by prolonged high temperatures and whether *ELF3* alleles may differ in these responses, suggesting a functional role for *ELF3* in later vegetative growth and development. To obtain phenotypic data for barley plants in a non-destructive manner, we developed an image-based phenotyping platform based on Raspberry 400 Pi computers and cameras (Fig. 4A) (Tovar *et al.*, 2018). Using this platform, we were able to image plants from three directions (two side-views separated by 90° and a top-view) simultaneously (Fig. 4A). Plant traits such as plant height, plant area, and convex hull area were extracted from the obtained images (Fig. 4B). The extracted values displayed a strong correlation with the manually measured values during the experiment (Fig. 4C), demonstrating the robustness of the imag- 405 ing and image analysis pipelines.

Zhu *et al.* (2022) Barley *ELF3* alleles tune phenotypic plasticity in response to high temperature

Starting from 8 DAS, each plant was imaged every two to four days to obtain growth curves under 20°C or 28°C treatment (Fig. 5). In confirmation of the above-described results (Fig. 3A; Supplementary Table S2), we observed a similar effect of temperature on plant height during the first two  
410 weeks of cultivation, lasting until around 30 DAS in all genotypes (Fig. 5A; Supplementary Table S4). However, after that, the positive effect of high temperature on plant height diminished and plants grown at 20°C were of similar size or even taller than those grown at 28°C (Fig. 5A; Supplementary Table S4). Although the time point when the 20°C grown plants surpassed the 28°C  
415 grown plants was genotype dependent, on 52 DAS, all genotypes displayed greater plant height at 20°C (Fig. 5A; Supplementary Table S4). These results are in line with previously reported negative effects of high temperature on plant height at maturity (Abou-Elwafa and Amein, 2016). Considering the allelic effects of *ELF3*, both the *elf3<sup>BW290</sup>* mutant as well as the 10\_wild allele surpassed their corresponding control lines (Bowman, 10\_elite) after 31 and 38 DAS, respectively, under both temperature treatments (Fig. 5A; Supplementary Table S4). In contrast, in HIF pairs 16  
420 and 17, the elite and exotic *ELF3* alleles did not display remarkable differences in plant height, with mainly temperature effects observed (Fig. 5A; Supplementary Table S4).

Similar to plant height, we observed reduced plant area at elevated temperatures at 52 DAS, except for HIF pair 16 showing no difference between temperatures (Fig. 5B; Supplementary Table  
425 S5). Albeit greater in plant height, the plant area of *elf3<sup>BW290</sup>* was smaller than Bowman from 45 DAS at 20°C and from 35 DAS at 28°C (Fig. 5B; Supplementary Table S5). However, plant area of 10\_elite and 10\_wild plants did not differ at 20°C, but only at 28°C (Fig. 5B; Supplementary Table S5). In general, from 42 DAS, *elf3<sup>BW290</sup>* and 10\_wild at 28°C displayed lowest plant areas from both top- and side-views among all genotypes (Fig. 5B; Supplementary Fig. S3A; Supplementary Ta-  
430 bles S5, S6). As such, extended elongation growth seems to come at the cost of reduced leaf area for light interception and photosynthesis, which likely depends on *ELF3*. To represent plant biomass, the plant volume was estimated based on the plant areas of top- and two side-views, showing similar trends as plant areas (Fig. 5C; Supplementary Table S7).

435 Interestingly, although plant area was reduced in *elf3<sup>BW290</sup>* and 10\_wild at 28°C, we observed relatively high convex hull areas from both top- and side views, especially in 10\_wild (Fig. 5D; Supplementary Fig. S3B; Supplementary Tables S8, S9). The convex hull area (the area of the red polygon in Fig. 4B) represents the smallest area enclosing the whole plant silhouette. Different to plant area, the convex hull area is mainly contributed by leaf length and bolting, representing the expansion of plants. Using both parameters (area and convex hull area) allowed a more comprehensive  
440 description of plant architecture. Our observations of reduced plant area but increased or stable convex hull area in *elf3<sup>BW290</sup>* and 10\_wild at 28°C could be a consequence of thinner leaves at 28°C (Fig. 3D; Supplementary Table S3). This conclusion is generally acceptable as the total tiller num-

Zhu *et al.* (2022) Barley *ELF3* alleles tune phenotypic plasticity in response to high temperature

ber on 52 DAS was not different (*elf3<sup>BW290</sup>*, HIF pair 10, 16\_elite and 17\_elite) or even higher (Bow-  
445 man, 16\_wild and 17\_wild) at 28°C (Fig. 6A; Supplementary Table S10). The larger convex hull  
area is a proxy for a more openly structured habitus of the shoot. From work in Arabidopsis it is  
known that such loose architectural adjustments promote ventilation and thereby facilitate evapora-  
tive leaf cooling at elevated temperatures (Crawford *et al.*, 2012).

450 To assess the overall phenotypic responses to elevated temperatures during vegetative growth  
and development, a principal component analysis (PCA) was carried out based on the arithmetic  
means of all obtained traits (Supplementary Fig. S4A). The first two principal components (PC1  
and PC2) accounted for 75.8% of the variance. PC1 separated samples by temperature treatment,  
whereas PC2 separated samples by genotype. While *elf3<sup>BW290</sup>* displayed a clear divergence of from  
455 other genotypes at both temperatures, this separation was observed in 10\_wild only at 28°C (Sup-  
plementary Fig. S4A). To avoid a potential bias in correlation caused by large amounts of non-sig-  
nificant data as part of the growth curve measured during early vegetative stage, we performed an  
additional PCA based on the growth curve modeling traits (Supplementary Fig. S4B). Using de-  
rived modeling traits, we were able to tone down the wealth of data and focus on important time  
460 points (e.g., day of maximum increase, day of maximum value, and end point) as well as general  
patterns of the growth curves (e.g., total area under the curve) instead of considering all measure-  
ment time points identically in the analysis. Again, clustering of *elf3<sup>BW290</sup>* and 10\_wild at 28°C was  
detected (Supplementary Fig. S4B).

465 Taken together, our data so far demonstrate that the Syrian *ELF3* allele in HIF pair 10 and *elf3<sup>BW290</sup>*  
mutant tend to behave similarly during vegetative growth and development. We can therefore con-  
clude that *ELF3* in general but also naturally occurring genetic variation in wild barley populations  
contribute to architectural changes of shoot tissues at elevated temperatures. Similar behavior of  
the exotic 10\_wild allele and the *ELF3* loss-of-function mutant *elf3<sup>BW290</sup>* (which carries a truncated  
470 *ELF3* protein due to a premature STOP codon) poses the question of functionality of the encoded  
protein variant 10\_wild, which is, however, out of the scope of this study.

### **An exotic *ELF3* allele accelerates barley developmental growth at elevated temperatures**

The plant life cycle can be divided into distinct phases from germination to senescence, and the  
475 timing of transition from one phase to the next can be either accelerated or delayed by high tem-  
peratures, depending on plant species and temperature regimes (reviewed in Lippmann *et al.*,  
2019). We therefore asked whether exotic *ELF3* alleles are involved in controlling developmental  
timing of leaf senescence and flowering at elevated temperatures. As chlorophyll degradation is  
one of the hallmarks of leaf senescence (Guo *et al.*, 2021), we monitored the chlorophyll content of  
480 the second leaf every week during the extended vegetative growth and development experiment



Zhu *et al.* (2022) Barley *ELF3* alleles tune phenotypic plasticity in response to high temperature

(Fig. 6B; Supplementary Table S11). As expected, we observed that all genotypes displayed earlier leaf senescence at 28°C compared to 20°C (Fig. 6B; Supplementary Table S11). Although the decrease of chlorophyll content was not *ELF3* dependent, we observed earlier onset of leaf senescence at both temperatures in HIF pairs 16 and 17, indicating an effect of the genetic background in these lines outside of the *ELF3* locus (Fig. 6B; Supplementary Table S11). Consistent with previous reports from various species (Djanaguiraman and Prasad, 2010; Lobell *et al.*, 2012; Shirdelmoghanloo *et al.*, 2016), our data suggest premature leaf senescence at elevated temperatures (Fig. 6B; Supplementary Table S11), but argues against a role of *ELF3* in its regulation.

Senescence of old leaves enables remobilization and retranslocation of nutrients to newly formed organs (e.g., sink leaves or seeds), and often correlates with the timing of flowering (Kim *et al.*, 2020). To test whether and how flowering time is affected by elevated temperatures and *ELF3* alleles, we scored the days until flag leaf sheath opening (BBCH-47, Fig. 6C) and the days until heading as a proxy for flowering time (BBCH-49, Fig. 6D). In contrast to *Arabidopsis*, but consistent with a previous report in barley (Ejaz and von Korff, 2017), we observed that Bowman displayed delayed flag leaf sheath opening and heading at 28°C compared to 20°C, whereas *elf3<sup>BW290</sup>* displayed the opposite temperature effect (Fig. 6C, D). Although 10\_elite plants did not finish flowering at both temperatures until the end of the experiment (62 DAS, data therefore omitted from Fig. 6C, D), 10\_wild plants flowered much earlier (Fig. 6D, E). Interestingly, the early flowering of 10\_wild plants was further accelerated by elevated temperatures, displaying an even larger temperature response compared to *elf3<sup>BW290</sup>* (Fig. 6D, E). The early flowering of *elf3<sup>BW290</sup>* and 10\_wild at 28°C indicates early bolting, which could partially explain previously observed architectural changes of these two lines (Fig. 5; Fig. 6C-E; Supplementary Figs. S3, S4; Supplementary Tables S4-9). In addition, the flowering time of 17\_wild was not temperature dependent (Fig. 6D), whereas the other genotypes (HIF pair 16 and 17\_elite) did not start flowering until the end of the experiment (data therefore omitted from Fig. 6C, D). Taken together, in the vast majority of phenotypes the sister lines of HIF pair 10 differed. We therefore focused further analyses on these genotypes.

To better understand the differences in the timing of vegetative to reproductive phase transition between the elite and wild alleles of HIF pair 10, we first assessed the allelic effects on barley meristem development and found that from 19 DAS, 10\_wild plants displayed faster inflorescence development than 10\_elite at both temperatures (Fig. 7A). In contrast to 10\_elite, the meristem development of 10\_wild was drastically accelerated by elevated temperatures, consistent with the flowering time results (Fig. 6C-E; Fig. 7A). To substantiate these observations on the molecular and regulatory level, we investigated the transcriptional behaviour of floral regulator genes in leaf samples from the plants used for meristem dissection (Fig. 7A, B; Supplementary Table S12). With few exceptions, transcript abundance of *Ppd-H1*, *FT1*, and *VRN1* remained largely unaltered by tem-



15 Zhu *et al.* (2022) Barley *ELF3* alleles tune phenotypic plasticity in response to high temperature

perature or *ELF3* allele (Fig. 7B; Supplementary Table S12). The exceptions were that 10\_elite at 28°C had reduced transcript levels of *Ppd-H1* (19 to 27 DAS) and *VRN1* (27 DAS) compared to 20°C, and 10\_wild at 28°C displayed reduced transcript levels of *Ppd-H1* and *FT1* on 40 DAS (Fig. 7B; Supplementary Table S12). During meristem development, transcript abundance of MADS-box genes *BM3* and *BM8* increased in both lines and temperature conditions (Fig. 7B; Supplementary Table S12). However, the onset of *BM3* and *BM8* expression occurred already at 19 DAS in 10\_wild at 28°C, which is earlier compared to 10\_wild at 20°C and 10\_elite (Fig. 7B; Supplementary Table S12). Correlated with flowering time and meristem development (Fig. 6C-E; Fig. 7A), 10\_wild plants displayed induced expression of *BM3* and *BM8* at 28°C between 19 to 33 DAS, when compared to 10\_elite under the same conditions (for *BM3*), or 10\_wild at 20°C (for *BM8*) (Fig. 7B; Supplementary Table S12), in line with the time points displaying morphological differences in shoot apical meristems displayed in Fig. 7A. Importantly, across development *ELF3* transcript levels hardly varied between both alleles in the vast majority of time points (Fig. 7B; Supplementary Table S12). Moreover, ~1.2 kb of promoter sequence upstream of the *ELF3* start codon was identical between both alleles (Supplementary Dataset S1), suggesting that the observed phenotypes including the differences in transcript abundance of downstream target genes are due to post-transcriptional differences between both alleles, possibly on the level of functional protein.

Together, flowering time data, floral meristem dissection and gene expression analyses demonstrate that the exotic *ELF3* allele in HIF pair 10 accelerates barley developmental growth at elevated temperatures, putatively by promoting the transcript levels of floral regulators including *BM3* and *BM8* MADS-box genes.

### **An exotic *ELF3* allele has reduced yield loss at elevated temperatures**

Under climate change scenarios, crop production and grain yield are predicted to be severely threatened by rising temperatures (Battisti and Naylor, 2009; Asseng *et al.*, 2015). With ambient temperature increased by 7 to 8°C, striking yield losses were observed in barley (Ejaz and von Korff, 2017; Ochagavía *et al.*, 2021). Interestingly, the early flowering mutant *elf3<sup>BW290</sup>* was reported to maintain seed number at elevated temperatures (Ejaz and von Korff, 2017; Ochagavía *et al.*, 2021), thereby representing some sort of increased yield stability. Since (i) the exotic *ELF3* allele in HIF pair 10 behaved similar to *elf3<sup>BW290</sup>* in many of the assays performed so far and (ii) to assess the effect of 10\_wild on yield at elevated temperatures, we performed an additional experiment in the greenhouse. In this experiment, four genotypes (Bowman, *elf3<sup>BW290</sup>*, and HIF pair 10) were grown in LD with day/night temperatures of 20°C/16°C (20°C treatment) or 28°C/24°C (28°C treat-

Zhu *et al.* (2022) Barley *ELF3* alleles tune phenotypic plasticity in response to high temperature

555 ment). To avoid the effects of elevated temperatures on early seedling establishment (Fig. 3; Sup-  
plementary Fig. S2; Supplementary Tables S2, S3), the temperature treatments started from the  
three-leaf stage (BBCH-13, 15 to 17 DAS) (Lancashire *et al.*, 1991). We first examined whether the  
growth and developmental traits under greenhouse conditions were comparable to the results from  
the environmentally better controlled phytochamber experiments. Despite the expected generally  
560 delayed phase transition under greenhouse conditions, we observed early flowering in *elf3<sup>BW290</sup>* at  
both temperatures and in 10\_wild at 28°C (Supplementary Fig. S5A); all four genotypes displayed  
reduced plant height at 28°C 118 DAS (Supplementary Fig. S5B). Total tiller number was not  
changed in Bowman but reduced in *elf3<sup>BW290</sup>* at elevated temperatures 118 DAS (Supplementary  
Fig. S5C). In contrast, both lines in HIF pair 10 had more tillers at 28°C than 20°C (Supplementary  
565 Fig. S5C). Taken together, although the total tiller number data were different (Fig. 6A; Supple-  
mentary Fig. S5C; Supplementary Table S10), the vast majority of phenotypes from the  
phytochamber experiments was reproducible in the greenhouse (Figs. 5A, 6A, C-E, 7; Supplemen-  
tary Fig. S5A, B; Supplementary Tables S4, S12). This suggested that documentation of yield re-  
lated phenotypes in the greenhouse may as well provide reliable insight into the roles of *ELF3* and  
570 especially the exotic 10\_wild allele.

At maturity, we measured plant dry weight, several spike parameters (ear length and grains/florets  
per spike), and several grain parameters (grain number, grain area, thousand grain weight, and  
grain yield) (Fig. 8; Supplementary Fig. S5D-F). We found plant dry weight to be reduced in Bow-  
575 man and 10\_elite at elevated temperatures, but it was not influenced by temperature in *elf3<sup>BW290</sup>*  
and 10\_wild (Fig. 8A). Under both temperatures, plant dry weight was lower in *elf3<sup>BW290</sup>* and  
10\_wild when compared to Bowman and 10\_elite, respectively (Fig. 8A). The ear length of Bow-  
man and *elf3<sup>BW290</sup>* was not affected by temperature, with *elf3<sup>BW290</sup>* having shorter ears than Bowman  
(Supplementary Fig. S5D). Shorter ears were also observed in 10\_wild compared to 10\_elite, but  
580 only at elevated temperatures (Supplementary Fig. S5D). At 28°C, the number of grains and florets  
per spike was reduced in Bowman, 10\_elite, and 10\_wild, but not in *elf3<sup>BW290</sup>* (Fig. 8B; Supplemen-  
tary Fig. S5E). The *elf3<sup>BW290</sup>* phenotype was consistent with the previous report from (Ejaz and von  
Korff, 2017). *elf3<sup>BW290</sup>* had less grains and florets per spike than Bowman under both temperatures,  
whereas 10\_wild only showed reduced grain and floret numbers per spike at 28°C compared to  
585 10\_elite (Fig. 8B; Supplementary Fig. S5E). The ratio of grains and florets per spike was slightly  
reduced in 10\_elite and 10\_wild at 28°C (Supplementary Fig. S5F), indicating the negative effects  
of high temperature on floret fertility as previously reported for wheat (Prasad and Djanaguiraman,  
2014).

590 The total grain number per plant displayed similar trends as the number of grains per spike, except  
that 10\_wild had reduced total grain number at 20°C (Fig. 8B, C). These results could be explained

Zhu *et al.* (2022) Barley *ELF3* alleles tune phenotypic plasticity in response to high temperature

by reduced spike or reproductive tiller number, as the total tiller number was not different in 10\_wild compared to 10\_elite at 20°C (Supplementary Fig. S5C). The grain area was not affected by temperature in Bowman and *elf3<sup>BW290</sup>*, with *elf3<sup>BW290</sup>* having smaller grain area compared to Bowman (Fig. 8D). In contrast, 10\_elite and 10\_wild displayed the same grain area which is reduced at elevated temperatures (Fig. 8D). The thousand grain weight (TGW) was not affected by temperature in Bowman, *elf3<sup>BW290</sup>* and 10\_elite, whereas 10\_wild had reduced TGW at elevated temperatures (Fig. 8E). The reduction in TGW of 10\_wild at 28°C resulted in reduced yield per plant, whereas the yield of the other lines was mostly dependent on the number of grains per plant (Fig. 8C, E, F). Albeit 10\_wild displayed striking yield loss at 20°C compared to 10\_elite, the yield of these two lines was not different at 28°C (Fig. 8F). These data suggest that the yield loss caused by elevated temperatures are mainly due to reduced grain number, which is mitigated in HIF pair 10 with the exotic *ELF3* allele.

To understand whether the yield parameters are linked to morphological and/or developmental traits, we analyzed putative correlations of temperature responses amongst all traits in Bowman, *elf3<sup>BW290</sup>*, and HIF pair 10 (Supplementary Dataset S2). Pairwise correlations of selected traits are shown in Fig. 9. As expected, high correlations can be observed among traits within similar growth and developmental stages. During early vegetative stage, temperature-induced leaf and tiller formation correlated strongly with early plant architectural traits (e.g., convex hull area, area, and volume, 16 DAS, Fig. 9). Similarly, temperature-induced reduction in yield strongly correlated with grain number, plant dry weight, as well as late plant architectural traits (e.g., area and volume, 52 DAS, Fig. 9). Interestingly, although temperature response of TGW was not correlated with any other yield parameters, it correlated positively with late plant architectural traits but negatively with early plant architectural traits (Fig. 9). These correlation patterns indicate potential connections of traits in barley response to elevated temperatures.

Taken together, our data demonstrate that an exotic barley *ELF3* allele not only contributes to thermomorphogenic architectural adjustments during vegetative growth, but also accelerates phase transition at elevated temperatures, mitigating further yield loss.

## Discussion

As global temperature is predicted to keep increasing in the near term, generating temperature-resilient crop varieties becomes an urgent need to avoid yield loss. Key regulators that provide phenotypic and developmental plasticity in response to elevated temperatures are poorly understood in major staple crops like barley. In this study, we systematically analyzed the effects of elevated

Zhu *et al.* (2022) Barley *ELF3* alleles tune phenotypic plasticity in response to high temperature

630 temperatures across the barley life cycle, including seedling establishment, vegetative to reproductive stage transition, and yield at maturity. Using HIF pairs generated from a segregating mapping population with wild or elite *ELF3* alleles but an otherwise largely fixed genomic background allowed us to study the role of naturally occurring genetic variation in *ELF3* in barley thermomorphogenesis across a full life cycle. Here, we demonstrate that an exotic *ELF3* allele interacts with high ambient temperature to accelerate growth and development in barley as an acclimation response, improving yield stability.

635

Thermomorphogenesis as a developmental process has been neglected for a long time. But studies in the model organism *Arabidopsis* and elucidation of the underlying regulatory mechanisms have significantly advanced the field in the last 25 years (Gray *et al.*, 1998; Delker *et al.*, 2022). In the model plant, elevated temperatures induce elongation of hypocotyl, petioles, as well as leaf hyponasty (Crawford *et al.*, 2012; Quint *et al.*, 2016; Park *et al.*, 2019). The barley lines used in our study likewise displayed increased plant height (Figs. 1, 3A, 5A; Supplementary Tables S2, S4) and accelerated formation of leaves and tillers (Fig. 3C), which were coupled with reduced leaf width (Fig. 3D; Supplementary Table S3) and the absence of a coleoptile tiller (Supplementary Fig. S2). As these thermoresponsive phenotypes are consistent with previous reports in barley and wheat (Cannell, 1969; Huang and Taylor, 1993; Abou-Elwafa and Amein, 2016), we conclude that the general phenotypic responses to elevated ambient temperatures during early vegetative development seem to be largely conserved across species. During seedling establishment, the *elf3*<sup>BW290</sup> mutant allele and the exotic allele 10\_wild, which was derived from the HEB-25 mapping population (Maurer *et al.*, 2015), mainly interacted with temperature in controlling elongation growth (Figs. 1, 3A, 5A; Supplementary Tables S2, S4), again similar to *elf3* mutant phenotypes in *Arabidopsis*. Via its functions as a thermosensor (through its prion-like domain) and as a core component of the circadian clock, *Arabidopsis* ELF3 negatively controls thermomorphogenesis via PIF4 (Box *et al.*, 2015; Raschke *et al.*, 2015; Jung *et al.*, 2020; Zhu *et al.*, 2022). As elongation of cereal leaves likely employs different mechanisms than those of dicots (Fricke, 2002) and ortholog relationships between *Arabidopsis* and barley *PIFs* are not phylogenetically traceable, a major regulatory hub like PIF4 in *Arabidopsis* is unknown in barley. Therefore, any assumption about the regulatory level of thermomorphogenesis in barley would be purely speculative.

660 Upon prolonged exposure to high temperature, plant height, plant area, and estimated biomass were reduced (Fig. 5A-C; Supplementary Fig. S3; Supplementary Tables S4-7). In combination with tillering and accelerated flowering, these phenotypes collectively resulted in architectural changes in the *elf3*<sup>BW290</sup> mutant and 10\_wild (Figs. 5, 6A, C-E, 7A; Supplementary Figs. S3, S4; Supplementary Tables S4-10). Such architectural acclimation can be characterized as well-distributed and distanced plant organs (Fig. 6E), analogous to the open rosette structure in *Arabidopsis*,

Zhu *et al.* (2022) Barley *ELF3* alleles tune phenotypic plasticity in response to high temperature

665 which improves leaf cooling and maintains photosynthetic efficiency at elevated temperatures (Crawford *et al.*, 2012; Park *et al.*, 2019). Interestingly, *elf3<sup>BW290</sup>* displayed such architecture even at 20°C compared to Bowman (Fig. 6E; Supplementary Figs. S3, S4; Supplementary Tables S6, S9), comparable to the constitutively thermoresponsive long hypocotyls and petioles of Arabidopsis *elf3* mutants at 17-22°C (Jung *et al.*, 2020; Zhu *et al.*, 2022). These conserved architectural re-  
670 sponses across species suggest that barley *ELF3* might play a similar role in temperature responses in Arabidopsis and cereals. As cereals generally lack the thermosensory prion-like domain (Jung *et al.*, 2020), it remains unclear whether this also refers to temperature sensing.

As especially reproductive development is vulnerable to increasing temperature and ultimately ac-  
675 counts for plant yields, understanding the effects of high temperature on reproductive development has become a leading research topic in barley (Fjellheim *et al.*, 2014; Jacott and Boden, 2020). Although inflorescence development in barley is generally inhibited by high temperature (reviewed in Jacott and Boden, 2020) as observed in Bowman, transition to flowering was induced early by elevated temperatures in *elf3<sup>BW290</sup>* and 10\_wild (Figs. 6C-E, 7A; Supplementary Fig. S4A). The obser-  
680 vations of Bowman and *elf3<sup>BW290</sup>* are highly consistent with a previous report under similar conditions (Ejaz and von Korff, 2017). In contrast to the loss-of-function mutant *elf3<sup>BW290</sup>* with its truncated *ELF3* protein due to a premature STOP codon, only a single amino acid substitution differentiates the two alleles of HIF pair 10 (W669G, Fig. 2) (Zakhrabekova *et al.*, 2012; Zahn *et al.*, 2022, Preprint). As transcript levels of *ELF3* remained unchanged under diurnal conditions be-  
685 tween the two sister lines in our previous experiments (Zahn *et al.*, 2022, Preprint), the W669G substitution may be responsible for functional differences on the protein level between the elite and wild alleles. And indeed, the W669G substitution was predicted to affect the secondary structure of *ELF3* protein, putatively disturbing protein-protein interactions (Zahn *et al.*, 2022, Preprint). Under diurnal conditions, *elf3<sup>BW290</sup>* promotes flowering by relieving the repression of *Ppd-H1* expression,  
690 whereas 10\_wild induces the transcript levels of *FT1* and *VRN1* without influencing the transcript levels of *Ppd-H1* (Ejaz and von Korff, 2017; Zahn *et al.*, 2022, Preprint). Surprisingly, we also observed almost no temperature effect on the transcript levels of *Ppd-H1*, *FT1*, and *VRN1* during inflorescence development (Fig. 7B; Supplementary Table S12). However, associated with meristem development, the transcript levels of floral inducer MADS-box genes *BM3* and *BM8* were induced  
695 by elevated temperatures exclusively in 10\_wild (Fig. 7; Supplementary Table S12). On the other hand, down-regulation of *BM3* and *BM8* was reported to be correlated with late flowering in sensitive lines responding to drought (Gol *et al.*, 2021). As under natural conditions, high temperature usually accompanies drought, these observations suggest a convergent responsive pathway. Considering the molecular connection between *ELF3* and *BM3/BM8*, gibberellin (GA) may be a poten-  
700 tial mediator. It was reported that constitutive early flowering of *elf3* mutants is a result of induced GA biosynthesis, which can be blocked by the GA inhibitor paclobutrazol (Boden *et al.*, 2014). In



20 Zhu *et al.* (2022) Barley *ELF3* alleles tune phenotypic plasticity in response to high temperature

addition to FT1, GA synthesized in leaves might act as a mobile signal, delivering florigenic information to the shoot apex to accelerate flowering (King and Evans, 2003). Similarly, in Arabidopsis GA biosynthesis is induced by high temperatures, and it has been suggested that bioactive GA  
705 contributes to thermomorphogenesis by delivering temperature signals from the root to the shoot via one of its precursors (Stavang *et al.*, 2009; Camut *et al.*, 2019). These results may provide insights for future research to study the role of GA in barley temperature response.

With its multiple functions, *ELF3* has been described as one of the key plasticity genes in plants  
710 (Laitinen and Nikoloski, 2019). Natural selection of these genes leads to the phenotypic and developmental plasticity enabling acclimation responses to changing environments (Blackman, 2017). In Arabidopsis, natural variation of *ELF3* has contributed to our understanding of its role in the circadian clock and thermomorphogenesis (Anwer *et al.*, 2014; Box *et al.*, 2015; Raschke *et al.*, 2015). To exploit barley natural variants of *ELF3* regarding temperature response, we selected three HIF  
715 pairs which have shown varying phenotypes between sister lines under field conditions and the exotic *ELF3* alleles of all three pairs carried W669G substitution in *ELF3* (Fig. 2) (Zahn *et al.*, 2022, Preprint). Surprisingly and in contrast to the above-described significant phenotypes of HIF pair 10, exotic *ELF3* alleles in HIF pairs 16 and 17 did not show a comparable temperature sensitivity (Figs. 3, 5; Supplementary Fig. S4; Supplementary Tables S2-9), although they carried four more  
720 amino acid substitutions in addition to the W669G replacement in *ELF3* (Fig. 2). This discrepancy suggests that our observations of HIF pair 10 rely on the interaction of *ELF3* with downstream genes *Ppd-H1* and/or *VRN1*. And indeed, while HIF pair 10 carries the wild allele of *Ppd-H1*, HIF pairs 16 and 17 have the elite *Ppd-H1*; HIF pair 16 also has the wild allele of *VRN1*, whereas HIF pairs 10 and 17 contain the elite *VRN1* (Supplementary Fig. S1) (Zahn *et al.*, 2022, Preprint).  
725 Therefore, the wild *Ppd-H1* in HIF pair 10 is likely a prerequisite for the temperature phenotypes caused by exotic *ELF3*, albeit its expression did not differ (Figs. 6C-E, 7B; Supplementary Fig. S4A). In addition, the interesting temperature-insensitive early flowering of 17\_wild could result from the interaction of exotic *ELF3* and elite *Ppd-H1* (Fig. 6C, D). Furthermore, the overall late flowering of HIF pair 16 (not flowered until the end of the experiment) can be explained by the wild  
730 *VRN1* (Fig. 6C, D). These hypotheses are supported by previous reports showing allelic effects of *Ppd-H1* and *VRN1* in barley temperature response (Ejaz and von Korff, 2017; Ochagavía *et al.*, 2021). These data emphasize the complex interactions of *ELF3* with photoperiod and vernalization pathways in barley flowering control at elevated temperatures, which deserve to be studied in more detail in the future.

735 Besides the scientific interest in flowering time regulation, the ultimate goal of plant production under global warming conditions is to prevent yield loss at elevated temperatures. Consistent with previous reports (Dias and Lidon, 2009; Ejaz and von Korff, 2017; Ochagavía *et al.*, 2021), we ob-



Zhu *et al.* (2022) Barley *ELF3* alleles tune phenotypic plasticity in response to high temperature

served general negative effects of high temperature on several yield parameters (Fig. 8; Supplementary Fig. S4D-F). The number of grains was strongly affected by high temperature in Bowman and 10\_elite (Fig. 8C). However, the reduction in grain number was not observed in *elf3*<sup>BW290</sup> and 10\_wild, resulting in mitigated yield loss, which is potentially achieved by the nature of early flowering (Fig. 8C, F). Early flowering or early maturing is generally coupled with yield loss, due to reduced leaf area and time available for photosynthetic assimilate production, whereas it is also a strategy of plants to avoid upcoming seasonal stressful conditions such as drought and heat in summer (Shavrukov *et al.*, 2017). Under global warming scenarios, various species flower much earlier, and this trend is predicted to continue, which indicates early flowering being an adaptive response (Parmesan and Yohe, 2003; Zheng *et al.*, 2016; Büntgen *et al.*, 2022). Providing further evidence, the short life cycle of *elf3*<sup>BW290</sup> and 10\_wild in our study at elevated temperatures is also characterized by open canopy architectures and increased yield stability (Figs. 3, 5, 6C-E, 8C-F; Supplementary Fig. S3; Supplementary Tables S2-9). Our data therefore establish *ELF3* as a potentially important player contributing to barley phenotypic and developmental acclimations to elevated temperatures. While the mechanistic consequences of allelic *ELF3* variants require extensive molecular studies, the presence of conditional phenotypic effects of exotic *ELF3* variants in response to elevated ambient temperatures encourages systematic exploitation of this genetic resource for breeding of climate resilient crops.

## Supplementary data

760 **Fig. S1.** Genomic setup of the used HIFs.

**Fig. S2.** Percentage of plants with coleoptile tillers (T0).

**Fig. S3.** Effects of exotic *ELF3* alleles and elevated temperatures on barley side-view plant area and architecture.

**Fig. S4.** Principal component analysis (PCA) of traits in growth and development experiment.

765 **Fig. S5.** Growth and development phenotypes, and spike parameters in the yield experiment.

**Table S1.** Sequences of primers used in this study.

**Table S2.** Plant height during early growth of barley seedlings (related to Fig. 3A).

**Table S3.** Length and width of the first and second leaves (related to Fig. 3D).

**Table S4.** Plant height during barley growth and development (related to Fig. 5A).

770 **Table S5.** Top-view plant area during barley growth and development (related to Fig. 5B).

**Table S6.** Side-view plant area during barley growth and development (related to Fig. S2A).

**Table S7.** Plant volume during barley growth and development (related to Fig. 5C).

**Table S8.** Top-view convex hull area during barley growth and development (related to Fig. 5D).

**Table S9.** Side-view convex hull area during barley growth and development (related to Fig. S2B).

Zhu *et al.* (2022) Barley *ELF3* alleles tune phenotypic plasticity in response to high temperature

775 **Table S10.** Total tiller number during barley growth and development (related to Fig. 6A).

**Table S11.** Chlorophyll content in the second leaf during barley growth and development (related to Fig. 6B).

**Table S12.** Transcript levels of barley flowering genes during growth and development (related to Fig. 7B).

780 **Dataset S1.** Promoter sequences of *ELF3* in HIF pair 10.

**Dataset S2.** Correlation of temperature responses amongst all traits.

## Acknowledgements

785 We thank Tanja Zahn for generating the plant material, and Carolin Delker for providing feedback on correlation analysis. We also thank Annette Pahlich, Martin Koch, and Danny Denks for their assistance in the yield experiment and Matthias Reimers for qPCR support.

## 790 Author contributions

KP and MQ conceived the study; ZZ and FE performed the growth and development experiment; SB performed the temperature assay on plates; ZZ and JT performed the gene expression analysis and meristem imaging; ZZ and AS performed the yield experiment; ZZ, FE, and SB sequenced *ELF3* in HIF pairs; AM performed growth curve modeling, PCA, and correlation analysis; ZZ wrote  
795 the manuscript; MQ edited the manuscript.

## Conflicts of interest

The authors declare that there is no conflict of interest.

800

## Funding

The funding of this work was provided by grants from the European Social Fund and the Federal State of Saxony-Anhalt (International Graduate School AGRIPOLY – Determinants of Plant Performance, grant no. ZS/2016/08/80644) to MQ.  
805

## Data availability statement

The data that support the findings of this study are available within the article and its supplementary data published online.  
810

## References

- Abou-Elwafa SF, Amein KA.** 2016. Genetic diversity and potential high temperature tolerance in barley (*Hordeum vulgare*). *World Journal of Agricultural Research* **4**, 1-8.
- 815 **Alvarez M, Tranquilli G, Lewis S, Kippes N, Dubcovsky J.** 2016. Genetic and physical mapping of the earliness per se locus *Eps-A m 1* in *Triticum monococcum* identifies EARLY FLOWERING 3 (*ELF3*) as a candidate gene. *Functional & Integrative Genomics* **16**, 365-382.
- Anand L, Rodriguez Lopez CM.** 2022. ChromoMap: an R package for interactive visualization of multi-omics data and annotation of chromosomes. *BMC bioinformatics* **23**, 1-9.
- 820 **Anwer MU, Boikoglou E, Herrero E, Hallstein M, Davis AM, James GV, Nagy F, Davis SJ.** 2014. Natural variation reveals that intracellular distribution of *ELF3* protein is associated with function in the circadian clock. *eLife* **3**, e02206.
- Aphalo PJ.** 2016. ggpmisc: An R package.
- 825 **Asseng S, Ewert F, Martre P, Rötter RP, Lobell DB, Cammarano D, Kimball BA, Ottman MJ, Wall G, White JW.** 2015. Rising temperatures reduce global wheat production. *Nature climate change* **5**, 143-147.
- Battisti DS, Naylor RL.** 2009. Historical warnings of future food insecurity with unprecedented seasonal heat. *Science* **323**, 240-244.
- 830 **Blackman BK.** 2017. Changing responses to changing seasons: natural variation in the plasticity of flowering time. *Plant Physiology* **173**, 16-26.
- Boden SA, Weiss D, Ross JJ, Davies NW, Trevaskis B, Chandler PM, Swain SM.** 2014. EARLY FLOWERING3 regulates flowering in spring barley by mediating gibberellin production and FLOWERING LOCUS T expression. *The Plant Cell* **26**, 1557-1569.
- 835 **Box MS, Huang BE, Domijan M, Jaeger KE, Khattak AK, Yoo SJ, Sedivy EL, Jones DM, Hearn TJ, Webb AA.** 2015. *ELF3* controls thermoresponsive growth in *Arabidopsis*. *Current Biology* **25**, 194-199.
- Büntgen U, Piermattei A, Krusic PJ, Esper J, Sparks T, Crivellaro A.** 2022. Plants in the UK flower a month earlier under recent warming. *Proceedings of the Royal Society B* **289**, 20212456.
- 840 **Campoli C, Shtaya M, Davis SJ, von Korff M.** 2012. Expression conservation within the circadian clock of a monocot: natural variation at barley *Ppd-H1* affects circadian expression of flowering time genes, but not clock orthologs. *BMC Plant Biology* **12**, 1-15.
- Camut L, Regnault T, Sirlin-Josserand M, Sakvarelidze-Achard L, Carrera E, Zumsteg J, Heintz D, Leonhardt N, Lange MJP, Lange T.** 2019. Root-derived GA12 contributes to temperature-induced shoot growth in *Arabidopsis*. *Nature Plants* **5**, 1216-1221.
- 845 **Cannell R.** 1969. The tillering pattern in barley varieties: II. The effect of temperature, light intensity and daylength on the frequency of occurrence of the coleoptile node and second tillers in barley. *The Journal of Agricultural Science* **72**, 423-435.
- Challinor AJ, Watson J, Lobell DB, Howden S, Smith D, Chhetri N.** 2014. A meta-analysis of crop yield under climate change and adaptation. *Nature climate change* **4**, 287-291.
- 850 **Chen Z, Galli M, Gallavotti A.** 2022. Mechanisms of temperature-regulated growth and thermotolerance in crop species. *Current Opinion in Plant Biology* **65**, 102134.
- Crawford AJ, McLachlan DH, Hetherington AM, Franklin KA.** 2012. High temperature exposure increases plant cooling capacity. *Current Biology* **22**, R396-R397.
- 855 **Dawson IK, Russell J, Powell W, Steffenson B, Thomas WT, Waugh R.** 2015. Barley: a translational model for adaptation to climate change. *New Phytologist* **206**, 913-931.
- Delker C, Quint M, Wigge PA.** 2022. Recent advances in understanding thermomorphogenesis signaling. *Current Opinion in Plant Biology* **68**, 102231.
- Delker C, van Zanten M, Quint M.** 2017. Thermosensing enlightened. *Trends in Plant Science* **22**, 185-187.
- 860 **Dias A, Lidon F.** 2009. Evaluation of grain filling rate and duration in bread and durum wheat, under heat stress after anthesis. *Journal of Agronomy and Crop Science* **195**, 137-147.
- Djanaguiraman M, Prasad PV.** 2010. Ethylene production under high temperature stress causes premature leaf senescence in soybean. *Functional Plant Biology* **37**, 1071-1084.

- 865 **Ejaz M, von Korff M.** 2017. The genetic control of reproductive development under high ambient temperature. *Plant Physiology* **173**, 294-306.
- Ezer D, Jung J-H, Lan H, Biswas S, Gregoire L, Box MS, Charoensawan V, Cortijo S, Lai X, Stöckle D.** 2017. The evening complex coordinates environmental and endogenous signals in *Arabidopsis*. *Nature Plants* **3**, 1-12.
- 870 **Faure S, Turner AS, Gruszka D, Christodoulou V, Davis SJ, von Korff M, Laurie DA.** 2012. Mutation at the circadian clock gene *EARLY MATURITY 8* adapts domesticated barley (*Hordeum vulgare*) to short growing seasons. *Proceedings of the National Academy of Sciences* **109**, 8328-8333.
- Fjellheim S, Boden S, Trevaskis B.** 2014. The role of seasonal flowering responses in adaptation of grasses to temperate climates. *Frontiers in Plant Science* **5**, 431.
- 875 **Ford B, Deng W, Clausen J, Oliver S, Boden S, Hemming M, Trevaskis B.** 2016. Barley (*Hordeum vulgare*) circadian clock genes can respond rapidly to temperature in an *EARLY FLOWERING 3*-dependent manner. *Journal of Experimental Botany* **67**, 5517-5528.
- Franklin KA, Lee SH, Patel D, Kumar SV, Spartz AK, Gu C, Ye S, Yu P, Breen G, Cohen JD.** 2011. Phytochrome-interacting factor 4 (*PIF4*) regulates auxin biosynthesis at high temperature. *Proceedings of the National Academy of Sciences* **108**, 20231-20235.
- 880 **Fricke W.** 2002. Biophysical limitation of cell elongation in cereal leaves. *Annals of Botany* **90**, 157-167.
- Fujita R, Ueno K, Yamazaki K.** 2000. The development of coleoptile tillers in relation to seedling vigor in early-maturing varieties of spring type wheat. *Plant production science* **3**, 275-280.
- 885 **Gol L, Haraldsson EB, von Korff M.** 2021. *Ppd-H1* integrates drought stress signals to control spike development and flowering time in barley. *Journal of Experimental Botany* **72**, 122-136.
- Gray WM, Östin A, Sandberg G, Romano CP, Estelle M.** 1998. High temperature promotes auxin-mediated hypocotyl elongation in *Arabidopsis*. *Proceedings of the National Academy of Sciences* **95**, 7197-7202.
- 890 **Guo Y, Ren G, Zhang K, Li Z, Miao Y, Guo H.** 2021. Leaf senescence: Progression, regulation, and application. *Molecular Horticulture* **1**, 1-25.
- Hartmann A, Czuderna T, Hoffmann R, Stein N, Schreiber F.** 2011. HTPHeno: an image analysis pipeline for high-throughput plant phenotyping. *BMC bioinformatics* **12**, 1-9.
- 895 **Hemming MN, Walford SA, Fieg S, Dennis ES, Trevaskis B.** 2012. Identification of high-temperature-responsive genes in cereals. *Plant Physiology* **158**, 1439-1450.
- Herrero E, Kolmos E, Bujdoso N, Yuan Y, Wang M, Berns MC, Uhlworm H, Coupland G, Saini R, Jaskolski M.** 2012. *EARLY FLOWERING4* recruitment of *EARLY FLOWERING3* in the nucleus sustains the *Arabidopsis* circadian clock. *The Plant Cell* **24**, 428-443.
- 900 **Huang B, Taylor HM.** 1993. Morphological development and anatomical features of wheat seedlings as influenced by temperature and seeding depth. *Crop Science* **33**, 1269-1273.
- Huang H, Nusinow DA.** 2016. Into the evening: Complex interactions in the *Arabidopsis* circadian clock. *Trends in Genetics* **32**, 674-686.
- Jacott CN, Boden SA.** 2020. Feeling the heat: developmental and molecular responses of wheat and barley to high ambient temperatures. *Journal of Experimental Botany* **71**, 5740-5751.
- 905 **Jung J-H, Barbosa AD, Hutin S, Kumita JR, Gao M, Derwort D, Silva CS, Lai X, Pierre E, Geng F.** 2020. A prion-like domain in *ELF3* functions as a thermosensor in *Arabidopsis*. *Nature* **585**, 256-260.
- Jung J-H, Domijan M, Klose C, Biswas S, Ezer D, Gao M, Khattak AK, Box MS, Charoensawan V, Cortijo S.** 2016. Phytochromes function as thermosensors in *Arabidopsis*. *Science* **354**, 886-889.
- 910 **Katoh K, Rozewicki J, Yamada KD.** 2019. MAFFT online service: multiple sequence alignment, interactive sequence choice and visualization. *Briefings in bioinformatics* **20**, 1160-1166.
- Kikuchi R, Kawahigashi H, Oshima M, Ando T, Handa H.** 2012. The differential expression of *HvCO9*, a member of the *CONSTANS*-like gene family, contributes to the control of flowering under short-day conditions in barley. *Journal of Experimental Botany* **63**, 773-784.
- 915 **Kim C, Kim SJ, Jeong J, Park E, Oh E, Park Y-I, Lim PO, Choi G.** 2020. High ambient temperature accelerates leaf senescence via *PHYTOCHROME-INTERACTING FACTOR 4* and *5* in *Arabidopsis*. *Molecules and cells* **43**, 645.



25 Zhu *et al.* (2022) Barley *ELF3* alleles tune phenotypic plasticity in response to high temperature

- 920 **King RW, Evans LT.** 2003. Gibberellins and flowering of grasses and cereals: prizing open the lid of the "florigen" black box. *Annual Review of Plant Biology* **54**, 307.
- Koini MA, Alvey L, Allen T, Tilley CA, Harberd NP, Whitelam GC, Franklin KA.** 2009. High temperature-mediated adaptations in plant architecture require the bHLH transcription factor PIF4. *Current Biology* **19**, 408-413.
- 925 **Kumar SV, Lucyshyn D, Jaeger KE, Alós E, Alvey E, Harberd NP, Wigge PA.** 2012. Transcription factor PIF4 controls the thermosensory activation of flowering. *Nature* **484**, 242-245.
- Laitinen RA, Nikoloski Z.** 2019. Genetic basis of plasticity in plants. *Journal of Experimental Botany* **70**, 739-745.
- Lancashire PD, Bleiholder H, Boom TVD, Langelüddeke P, Stauss R, Weber E, Witzemberger A.** 1991. A uniform decimal code for growth stages of crops and weeds. *Annals of applied Biology* 930 **119**, 561-601.
- Legris M, Klose C, Burgie ES, Rojas CCR, Neme M, Hiltbrunner A, Wigge PA, Schäfer E, Vierstra RD, Casal JJ.** 2016. Phytochrome B integrates light and temperature signals in Arabidopsis. *Science* **354**, 897-900.
- Leng G, Huang M.** 2017. Crop yield response to climate change varies with crop spatial distribution pattern. *Scientific Reports* **7**, 1-10.
- 935 **Li C, Lin H, Dubcovsky J.** 2015. Factorial combinations of protein interactions generate a multiplicity of florigen activation complexes in wheat and barley. *The Plant Journal* **84**, 70-82.
- Liang Y, Richards R.** 1994. Coleoptile tiller development is associated with fast early vigour in wheat. *Euphytica* **80**, 119-124.
- 940 **Lincoln C, Britton JH, Estelle M.** 1990. Growth and development of the *axr1* mutants of Arabidopsis. *The Plant Cell* **2**, 1071-1080.
- Lippmann R, Babben S, Menger A, Delker C, Quint M.** 2019. Development of wild and cultivated plants under global warming conditions. *Current Biology* **29**, R1326-R1338.
- Lobell DB, Sibley A, Ivan Ortiz-Monasterio J.** 2012. Extreme heat effects on wheat senescence 945 in India. *Nature climate change* **2**, 186-189.
- Lu S, Zhao X, Hu Y, Liu S, Nan H, Li X, Fang C, Cao D, Shi X, Kong L.** 2017. Natural variation at the soybean *J* locus improves adaptation to the tropics and enhances yield. *Nature genetics* **49**, 773-779.
- Maurer A, Draba V, Jiang Y, Schnaithmann F, Sharma R, Schumann E, Kilian B, Reif JC, Pillen K.** 2015. Modelling the genetic architecture of flowering time control in barley through nested association mapping. *BMC genomics* **16**, 1-12.
- Maurer A, Draba V, Pillen K.** 2016. Genomic dissection of plant development and its impact on thousand grain weight in barley through nested association mapping. *Journal of Experimental Botany* **67**, 2507-2518.
- 955 **Müller LM, Mombaerts L, Pankin A, Davis SJ, Webb AA, Goncalves J, von Korff M.** 2020. Differential effects of day/night cues and the circadian clock on the barley transcriptome. *Plant Physiology* **183**, 765-779.
- Newton AC, Flavell AJ, George TS, Leat P, Mullholland B, Ramsay L, Revoredo-Giha C, Russell J, Steffenson BJ, Swanston JS.** 2011. Crops that feed the world 4. Barley: a resilient crop? 960 Strengths and weaknesses in the context of food security. *Food security* **3**, 141-178.
- Ning Y, Shi X, Wang R, Fan J, Park CH, Zhang C, Zhang T, Ouyang X, Li S, Wang G-L.** 2015. OsELF3-2, an ortholog of Arabidopsis ELF3, interacts with the E3 ligase APIP6 and negatively regulates immunity against *Magnaporthe oryzae* in rice. *Molecular Plant* **8**, 1679-1682.
- Nusinow DA, Helfer A, Hamilton EE, King JJ, Imaizumi T, Schultz TF, Farré EM, Kay SA.** 965 2011. The ELF4–ELF3–LUX complex links the circadian clock to diurnal control of hypocotyl growth. *Nature* **475**, 398-402.
- Ochagavía H, Kiss T, Karsai I, Casas AM, Igartua E.** 2021. Responses of Barley to High Ambient Temperature Are Modulated by Vernalization. *Frontiers in Plant Science* **12**.
- Park Y-J, Lee H-J, Gil K-E, Kim JY, Lee J-H, Lee H, Cho H-T, Vu LD, De Smet I, Park C-M.** 970 2019. Developmental programming of thermonastic leaf movement. *Plant Physiology* **180**, 1185-1197.
- Parmesan C, Yohe G.** 2003. A globally coherent fingerprint of climate change impacts across natural systems. *Nature* **421**, 37-42.

Zhu *et al.* (2022) Barley *ELF3* alleles tune phenotypic plasticity in response to high temperature

- 975 **Prasad PV, Djanaguiraman M.** 2014. Response of floret fertility and individual grain weight of wheat to high temperature stress: sensitive stages and thresholds for temperature and duration. *Functional Plant Biology* **41**, 1261-1269.
- Quint M, Delker C, Franklin KA, Wigge PA, Halliday KJ, Van Zanten M.** 2016. Molecular and genetic control of plant thermomorphogenesis. *Nature Plants* **2**, 1-9.
- R Core Team.** 2013. R: A language and environment for statistical computing.
- 980 **Raschke A, Ibañez C, Ullrich KK, Anwer MU, Becker S, Glöckner A, Trenner J, Denk K, Saal B, Sun X.** 2015. Natural variants of *ELF3* affect thermomorphogenesis by transcriptionally modulating PIF4-dependent auxin response genes. *BMC Plant Biology* **15**, 1-10.
- Ridge S, Deokar A, Lee R, Daba K, Macknight RC, Weller JL, Tar'an B.** 2017. The chickpea Early Flowering 1 (*Efl1*) locus is an ortholog of Arabidopsis *ELF3*. *Plant Physiology* **175**, 802-815.
- 985 **Russell J, Dawson IK, Flavell AJ, Steffenson B, Weltzien E, Booth A, Ceccarelli S, Grando S, Waugh R.** 2011. Analysis of > 1000 single nucleotide polymorphisms in geographically matched samples of landrace and wild barley indicates secondary contact and chromosome-level differences in diversity around domestication genes. *New Phytologist* **191**, 564-578.
- Shavrukov Y, Kurishbayev A, Jatayev S, Shvidchenko V, Zotova L, Koekemoer F, De Groot S, Soole K, Langridge P.** 2017. Early flowering as a drought escape mechanism in plants: how can it aid wheat production? *Frontiers in Plant Science* **8**, 1950.
- 990 **Shirdelmoghanloo H, Taylor JD, Lohraseb I, Rabie H, Brien C, Timmins A, Martin P, Mather DE, Emebiri L, Collins NC.** 2016. A QTL on the short arm of wheat (*Triticum aestivum* L.) chromosome 3B affects the stability of grain weight in plants exposed to a brief heat shock early in grain filling. *BMC Plant Biology* **16**, 1-15.
- 995 **Stavang JA, Gallego-Bartolomé J, Gómez MD, Yoshida S, Asami T, Olsen JE, García-Martínez JL, Alabadí D, Blázquez MA.** 2009. Hormonal regulation of temperature-induced growth in Arabidopsis. *The Plant Journal* **60**, 589-601.
- Tovar JC, Hoyer JS, Lin A, Tielking A, Callen ST, Elizabeth Castillo S, Miller M, Tessman M, Fahlgren N, Carrington JC.** 2018. Raspberry Pi-powered imaging for plant phenotyping. *Applications in Plant Sciences* **6**, e1031.
- 1000 **Trevaskis B, Tadege M, Hemming MN, Peacock WJ, Dennis ES, Sheldon C.** 2007. Short vegetative phase-like MADS-box genes inhibit floral meristem identity in barley. *Plant Physiology* **143**, 225-235.
- 1005 **Turner A, Beales J, Faure S, Dunford RP, Laurie DA.** 2005. The pseudo-response regulator Ppd-H1 provides adaptation to photoperiod in barley. *Science* **310**, 1031-1034.
- Xia T, Zhang L, Xu J, Wang L, Liu B, Hao M, Chang X, Zhang T, Li S, Zhang H.** 2017. The alternative splicing of *EAM8* contributes to early flowering and short-season adaptation in a landrace barley from the Qinghai-Tibetan Plateau. *Theoretical and applied genetics* **130**, 757-766.
- 1010 **Zahn T, Zhu Z, Ritoff N, Krapf J, Junker A, Altmann T, Schmutzer T, Tueting C, Kastritis PL, Quint M, Pillen K, Maurer A.** 2022. Exotic alleles of *EARLY FLOWERING 3* determine plant development and grain yield in barley. *bioRxiv*, 2022.2007.2015.500212. [Preprint]
- Zakhrabekova S, Gough SP, Braumann I, Müller AH, Lundqvist J, Ahmann K, Dockter C, Matyszczyk I, Kurowska M, Druka A.** 2012. Induced mutations in circadian clock regulator *Mat-a* facilitated short-season adaptation and range extension in cultivated barley. *Proceedings of the National Academy of Sciences* **109**, 4326-4331.
- 1015 **Zhao C, Liu B, Piao S, Wang X, Lobell DB, Huang Y, Huang M, Yao Y, Bassu S, Ciais P.** 2017. Temperature increase reduces global yields of major crops in four independent estimates. *Proceedings of the National Academy of Sciences* **114**, 9326-9331.
- 1020 **Zheng B, Chenu K, Chapman SC.** 2016. Velocity of temperature and flowering time in wheat—assisting breeders to keep pace with climate change. *Global Change Biology* **22**, 921-933.
- Zhu Z, Quint M, Anwer MU.** 2022. Arabidopsis *EARLY FLOWERING 3* controls temperature responsiveness of the circadian clock independently of the evening complex. *Journal of Experimental Botany* **73**, 1049-1061.
- 1025



Zhu *et al.* (2022) Barley *ELF3* alleles tune phenotypic plasticity in response to high temperature

## Figure legends

**Figure 1.** *ELF3* is involved in the temperature response of barley seedlings. Bowman and *elf3*<sup>BW290</sup> seedlings were grown at constant 20 or 28°C in LD (16 h light/ 8 h dark) with light intensity of 90  $\mu\text{mol m}^{-2}\text{s}^{-1}$ . Leaf tips were marked after germination and the leaf length from the marked position was measured in two consecutive days. Boxes show medians and interquartile ranges. The whiskers extend to 1.5x interquartile ranges. Dots represent values of individual plants ( $n=9-17$ ). Different letters above the boxes indicate significant differences (small and capital letters for the first and second days, respectively, two-way ANOVA and Tukey's HSD test,  $P<0.05$ ).

1035

**Figure 2.** Variations in *ELF3* sequence among HIF pairs. Black rectangles (exons) and connecting lines (introns) represent the structure of barley *ELF3* (cv. Barke). Positions of the nonsynonymous single-nucleotide polymorphisms (SNPs) are shown as red vertical bars with corresponding amino acid substitutions shown above the scheme. Positions of the synonymous SNPs and the insertion-deletion mutations (Indels) in introns are shown as blue vertical bars. All mutations are listed in the table, using Barke sequence as reference. The sequence of the 104-bp-insertion at position 1989 is: AGCAA ATGAAT GAATCT AACTC TAAAT ATGTCT ATATAC ATCGTA TG TAGT CCACTA GTGGAA TCTCTA GAAAGA CTTATA TTTAGG AACGGA GGGAGT AT.

**Figure 3.** Elevated temperatures accelerate early growth and development of barley seedlings. Bowman, *elf3*<sup>BW290</sup> and HIF pairs were grown in LD (16 h light/ 8 h dark) at day/night temperatures of 20/16°C (20°C). At 5 days after sowing (DAS), seedlings were shifted to 28/24°C (28°C) or were kept at 20°C. (A) Plant height was measured manually on a daily basis. Lines represent the mean and ribbons indicate standard error of mean (SEM,  $n=11$ ). Hashtags (for Bowman and HIF elite lines with *HvELF3*) and asterisks (for *elf3*<sup>BW290</sup> and HIF wild lines with *HspELF3*) indicate significant differences between two temperature treatments (# and \*,  $P<0.05$ ; ## and \*\*,  $P<0.01$ ; ### and \*\*\*,  $P<0.001$ ; two-way ANOVA). (B) Schematic representation of a barley seedling in its three-leaf stage. (C) Days until visible third leaf (L3) and first tiller (T1). Boxes show medians and interquartile ranges. The whiskers extend to 1.5x interquartile ranges. Dots represent values of individual plants. Different letters above the boxes indicate significant differences (two-way ANOVA and Tukey's HSD test,  $P<0.05$ ). (D) Length and width of the first (circles) and second (squares) leaves ( $n=5$ ) in all genotypes at 16 DAS. The genotypic effect and multiple comparisons are shown in Supplementary Table S3.

**Figure 4.** Image-based plant phenotyping for the growth and development experiment. (A) Schematic representation of the phenotyping setup. At each imaging time, images of plants were simultaneously taken from three directions. Pi, a set of a Raspberry Pi microcomputer and an RGB

Zhu *et al.* (2022) Barley *ELF3* alleles tune phenotypic plasticity in response to high temperature

camera module with lighting. (B) Example of raw and output images from the image analysis pipeline. Raw images were analyzed for plant height, area, and convex hull area. Red polygon represents the convex hull with its circumcircle. (C) Linear regression of plant height values obtained from image analysis (x axis) and from manual measurement (y axis). All values ( $n=880$ ) obtained at 8, 16, 28, 35, and 49 DAS were plotted and used for linear regression.

**Figure 5.** Effects of exotic *ELF3* alleles and elevated temperatures on barley growth and plant architecture. (A-D) Bowman, *elf3<sup>BW290</sup>* and HIF pairs were grown in LD (16 h light/ 8 h dark) at day/night temperatures of 20/16°C (20°C). At 5 DAS, seedlings were shifted to 28/24°C (28°C) or were kept at 20°C. From 8 DAS, plants were imaged every two to four days. Plant height (A, average of two side-views) and top-view plant area (B) were obtained using HTPHeno pipeline. (C) Plant volume was estimated using plant area data from top-view (B) and two side-views. (D) Top-view convex hull area was obtained using Hull & Circle pipeline. Lines represent the mean and ribbons indicate SEM ( $n=11$ ). Hashtags (for Bowman and HIF elite lines with *HvELF3*) and asterisks (for *elf3<sup>BW290</sup>* and HIF wild lines with *HspELF3*) indicate significant differences between two temperature treatments (# and \*,  $P<0.05$ ; ## and \*\*,  $P<0.01$ ; ### and \*\*\*,  $P<0.001$ ; two-way ANOVA).

**Figure 6.** Effects of exotic *ELF3* alleles and elevated temperatures on barley tillering, leaf senescence, and heading. (A-E) Bowman, *elf3<sup>BW290</sup>* and HIF pairs were grown in LD (16 h light/ 8 h dark) at day/night temperatures of 20/16°C (20°C). At 5 DAS, seedlings were shifted to 28/24°C (28°C) or were kept at 20°C. (A) Total tiller number was scored from 14 DAS. (B) Chlorophyll content of the second leaf was measured every week from 16 DAS. Lines represent the mean and ribbons indicate SEM ( $n=11$ ). Hashtags (for Bowman and HIF elite lines with *HvELF3*) and asterisks (for *elf3<sup>BW290</sup>* and HIF wild lines with *HspELF3*) indicate significant differences between two temperature treatments (# and \*,  $P<0.05$ ; ## and \*\*,  $P<0.01$ ; ### and \*\*\*,  $P<0.001$ ; two-way ANOVA). Days until flag leaf sheath opening (C) and heading (D) were scored in the lines showing visible awns before the end of the experiment. Boxes show medians and interquartile ranges. The whiskers extend to 1.5x interquartile ranges. Dots represent values of individual plants. Different letters above the boxes indicate significant differences (two-way ANOVA and Tukey's HSD test,  $P<0.05$ ). (E) Representative images of Bowman, *elf3<sup>BW290</sup>*, 10\_elite, and 10\_wild plants on 38 DAS. Scale bar = 10 cm.

**Figure 7.** An exotic *ELF3* allele interacts with elevated temperatures to control meristem development and the transcript levels of flowering genes. (A) Representative images of shoot apex meristem and inflorescence in 10\_elite and 10\_wild plants grown in LD (16 h light/ 8 h dark) at day/night temperatures of 20/16°C (20°C). At 5 DAS, seedlings were shifted to 28/24°C (28°C) or were kept at 20°C. Three plants were harvested per genotype per temperature at 12, 19, 27, 33, and 40

Zhu *et al.* (2022) Barley *ELF3* alleles tune phenotypic plasticity in response to high temperature

1100 DAS. Figures in white boxes indicates Waddington scale scores until 6.0. Scale bars, white = 500  $\mu\text{m}$ ; red = 2 cm. (B) Transcript levels of barley flowering genes. Leaf samples were harvested at ZT08 during meristem dissection at each time point in (A), as well as at 5 DAS before the start of temperature treatment. Expression levels were normalized to *HvACTIN* and *HvGAPDH*. Error bars indicate the SEM ( $n=3$ ) of three biological replicates. Hashtags (for 10\_elite) and asterisks (for 1105 10\_wild) indicate significant differences between two temperature treatments (# and \*,  $P<0.05$ ; ## and \*\*,  $P<0.01$ ; ### and \*\*\*,  $P<0.001$ ; two-way ANOVA).

**Figure 8.** An exotic *ELF3* allele mitigates yield loss at elevated temperatures. Bowman, *elf3<sup>BW290</sup>*, and HIF pair 10 plants were grown in greenhouse conditions with LD (16 h light/ 8 h dark) and day/night temperatures of 20/16°C (20°C). Plants reached three-leaf stage were shifted to 28/24°C (28°C) or were kept at 20°C. At maturity, plant dry weight (A), number of grains per spike (B) and per plant (C), grain area (D), thousand grain weight (E), and yield per plant (F) were scored. Boxes show medians and interquartile ranges. The whiskers extend to 1.5x interquartile ranges. Dots represent values of individual plants ( $n=12-15$ ). Different letters above or below the boxes indicate significant differences (two-way ANOVA and Tukey's HSD test,  $P<0.05$ ). 1115

**Figure 9.** Correlation of temperature responses in selected traits. Pairwise correlation coefficients were determined for Bowman, *elf3<sup>BW290</sup>*, and HIF pair 10 between selected traits obtained from both growth and development, and yield experiments. Numbers in the bracket indicate DAS. Pearson correlation coefficients were tested for significance and only significant coefficients with  $P<0.05$  are not crossed. Correlations for all measured and derived growth curve modeling traits are shown in Supplementary Dataset S2. 1120

**Figure S1.** Genomic setup of the used HIFs. Comparison of two sister lines (upper chromosomes, elite line; lower chromosomes, wild line) in each HIF pair based on the genotype data generated from the Infinium iSelect 50k SNP chip (Zahn *et al.*, 2022, Preprint). Black regions were not covered in genotyping. Green and orange parts represent homozygous elite and wild regions, respectively, whereas yellow parts represent heterozygous locus. The arrows indicate *ELF3* locus on chromosome 1H. The additional seven major flowering time genes exhibited the same fixed homozygous alleles between sister lines in all three HIF pairs. Window scaling was based on length proportion and 200 windows were created for the longest chromosome. 1130

**Figure S2.** Percentage of plants with coleoptile tillers (T0). Bowman, *elf3<sup>BW290</sup>* and HIF pairs were grown in LD (16 h light/ 8 h dark) at day/night temperatures of 20/16°C (20°C). At 5 DAS, seedlings were shifted to 28/24°C (28°C) or were kept at 20°C. The formation of T0 was scored on 18 DAS ( $n=11$ ). 1135

**Figure S3.** Effects of exotic *ELF3* alleles and elevated temperatures on barley side-view plant area and architecture. (A, B) Bowman, *elf3<sup>BW290</sup>* and HIF pairs were grown in LD (16 h light/ 8 h dark) at day/night temperatures of 20/16°C (20°C). At 5 DAS, seedlings were shifted to 28/24°C (28°C) or were kept at 20°C. From 8 DAS, plants were imaged every two to four days. Side-view plant area (A) and convex hull area (B) were obtained using HTPPheno and Hull & Circle pipelines (average of two side-views). Lines represent the mean and ribbons indicate SEM ( $n=11$ ). Hashtags (for Bowman and HIF elite lines with *HvELF3*) and asterisks (for *elf3<sup>BW290</sup>* and HIF wild lines with *HspELF3*) indicate significant differences between two temperature treatments (# and \*,  $P<0.05$ ; ## and \*\*,  $P<0.01$ ; ### and \*\*\*,  $P<0.001$ ; two-way ANOVA).

**Figure S4.** Principal component analysis (PCA) of traits in growth and development experiment. (A, B) PCA was based on the correlation matrix using the arithmetic means of all obtained traits (A), or the derived growth curve modeling traits (B) from growth and development experiment.

**Figure S5.** Growth and development phenotypes, and spike parameters in the yield experiment. Bowman, *elf3<sup>BW290</sup>*, and HIF pair 10 plants were grown in greenhouse conditions with LD (16 h light/ 8 h dark) and day/night temperatures of 20/16°C (20°C). Plants reached three-leaf stage were shifted to 28/24°C (28°C) or were kept at 20°C. The developmental stage (A) was scored at 73 DAS, whereas plant height (B) and total tiller number (C) were scored at 118 DAS. The developmental stage of all *elf3<sup>BW290</sup>* plants at both temperatures were over BBCH-59 at 73 DAS. At maturity, the spike parameters: ear length (D), number of florets per spike (E), and grain/floret ratio (F) were scored. Boxes show medians and interquartile ranges. The whiskers extend to 1.5x interquartile ranges. Dots represent values of individual plants ( $n=12-15$ ). Different letters above or below the boxes indicate significant differences (two-way ANOVA and Tukey's HSD test,  $P<0.05$ ).

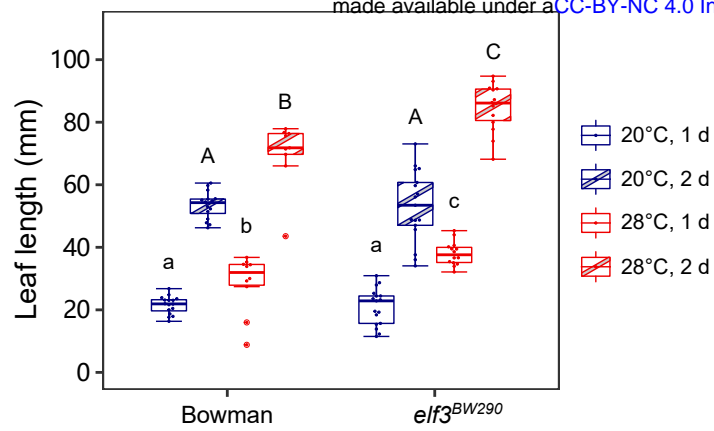


**Fig. 1.** *ELF3* is involved in the temperature response of barley seedlings. Bowman and *elf3*<sup>BW290</sup> seedlings were grown at constant 20 or 28°C in LD (16 h light/ 8 h dark) with light intensity of 90  $\mu\text{mol m}^{-2}\text{s}^{-1}$ . Leaf tips were marked after germination and the leaf length from the marked position was measured in two consecutive days. Boxes show medians and interquartile ranges. The whiskers extend to 1.5x interquartile ranges. Dots represent values of individual plants ( $n=9-17$ ). Different letters above the boxes indicate significant differences (small and capital letters for the first and second days, respectively, two-way ANOVA and Tukey's HSD test,  $P<0.05$ ).



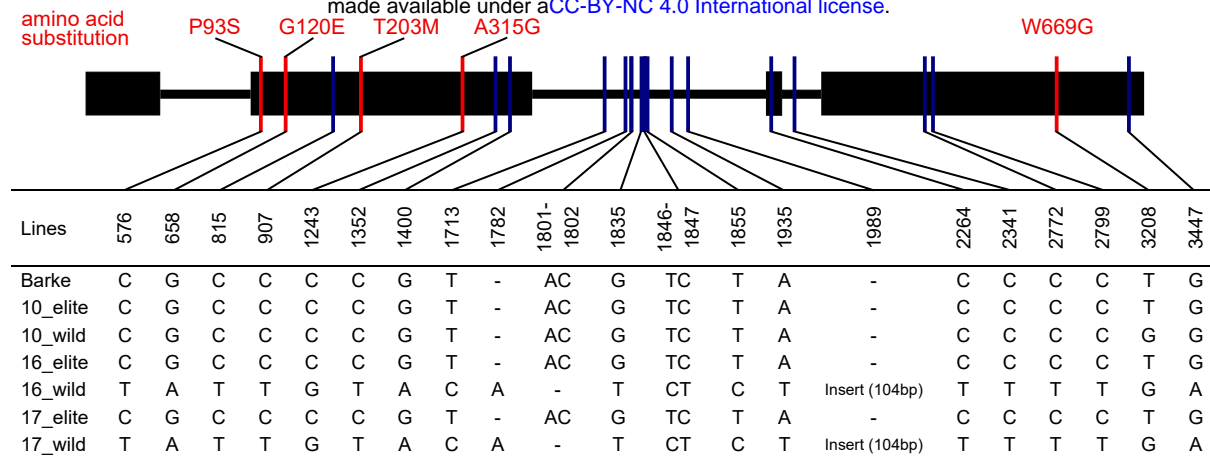


**Fig. 2.** Variations in *ELF3* sequence among HIF pairs. Black rectangles (exons) and connecting lines (introns) represent the structure of barley *ELF3* (cv. Barke). Positions of the nonsynonymous single-nucleotide polymorphisms (SNPs) are shown as red vertical bars with corresponding amino acid substitutions shown above the scheme. Positions of the synonymous SNPs and the insertion-deletion mutations (Indels) in introns are shown as blue vertical bars. All mutations are listed in the table, using Barke sequence as reference. The sequence of the 104-bp-insertion at position 1989 is: AGCAAATG AAT GAATCT ACACTC TAAAT ATGTCT ATATAC ATCGTA TGTAGT CCACTA GTGGAA TCTCTA GAA AGA CTTATA TTTAGG AACGGA GGGAGT AT.

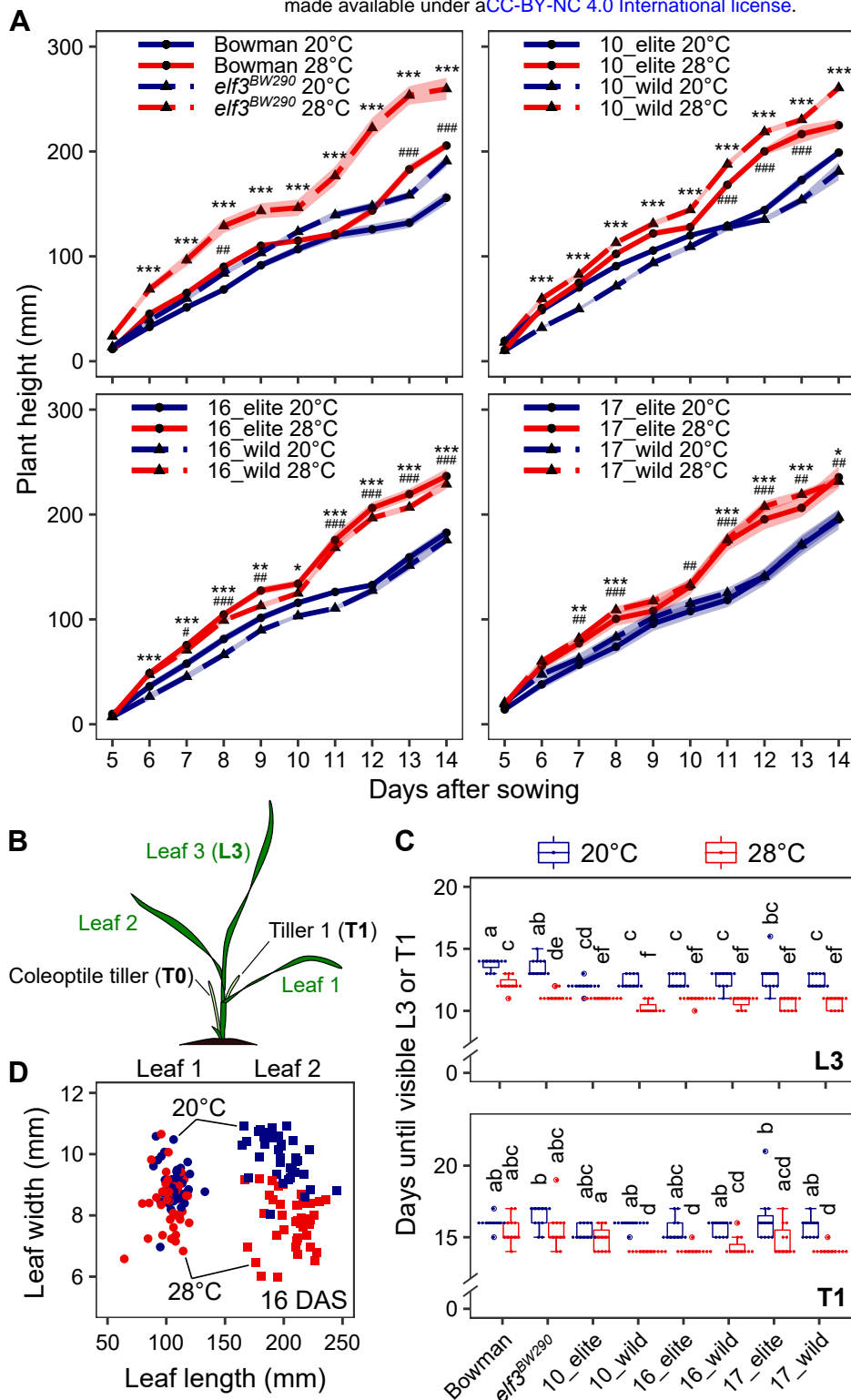


**Fig. 3.** Elevated temperatures accelerate early growth and development of barley seedlings. Bowman, *elf3<sup>BW290</sup>* and HIF pairs were grown in LD (16 h light/ 8 h dark) at day/night temperatures of 20/16°C (20°C). At 5 days after sowing (DAS), seedlings were shifted to 28/24°C (28°C) or were kept at 20°C. (A) Plant height was measured manually on a daily basis. Lines represent the mean and ribbons indicate standard error of mean (SEM,  $n=11$ ). Hashtags (for Bowman and HIF elite lines with *HvELF3*) and asterisks (for *elf3<sup>BW290</sup>* and HIF wild lines with *HspELF3*) indicate significant differences between two temperature treatments (# and \*,  $P<0.05$ ; ## and \*\*,  $P<0.01$ ; ### and \*\*\*,  $P<0.001$ ; two-way ANOVA). (B) Schematic representation of a barley seedling in its three-leaf stage. (C) Days until visible third leaf (L3) and first tiller (T1). Boxes show medians and interquartile ranges. The whiskers extend to 1.5x interquartile ranges. Dots represent values of individual plants. Different letters above the boxes indicate significant differences (two-way ANOVA and Tukey's HSD test,  $P<0.05$ ). (D) Length and width of the first (circles) and second (squares) leaves ( $n=5$ ) in all genotypes at 16 DAS. The genotypic effect and multiple comparisons are shown in Supplementary Table S3.

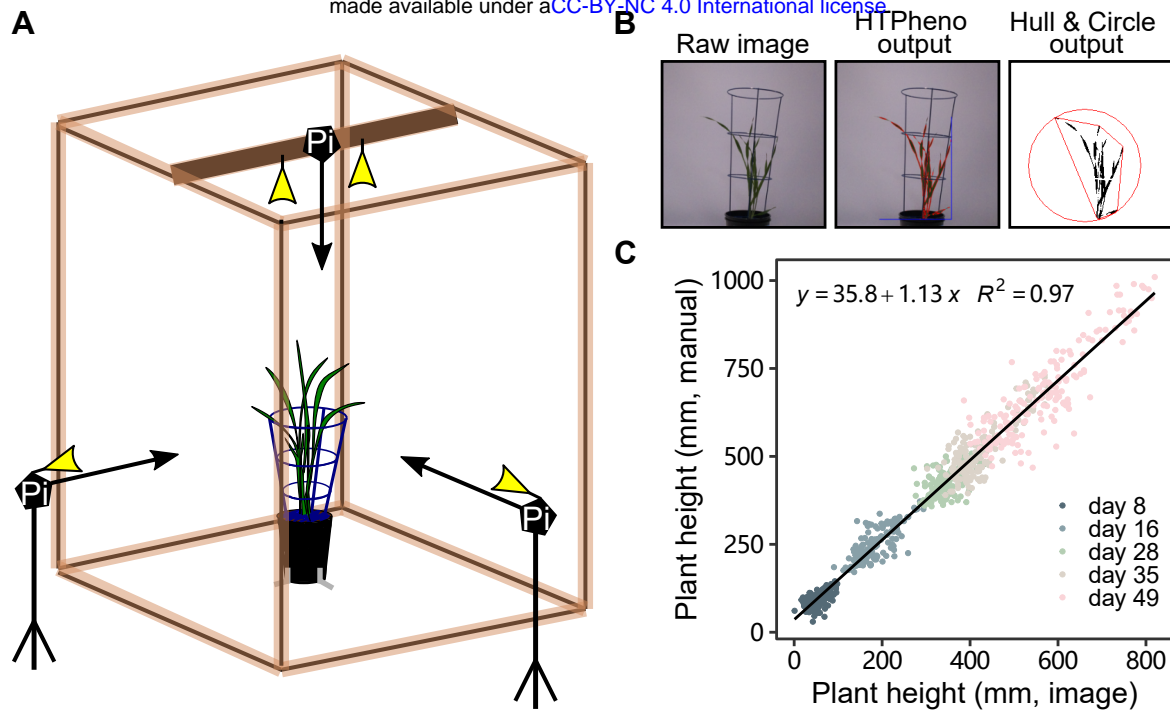


**Fig. 4.** Image-based plant phenotyping for the growth and development experiment. (A) Schematic representation of the phenotyping setup. At each imaging time, images of plants were simultaneously taken from three directions. Pi, a set of a Raspberry Pi microcomputer and an RGB camera module with lighting. (B) Example of raw and output images from the image analysis pipeline. Raw images were analyzed for plant height, area, and convex hull area. Red polygon represents the convex hull with its circumcircle. (C) Linear regression of plant height values obtained from image analysis (x axis) and from manual measurement (y axis). All values ( $n=880$ ) obtained at 8, 16, 28, 35, and 49 DAS were plotted and used for linear regression.

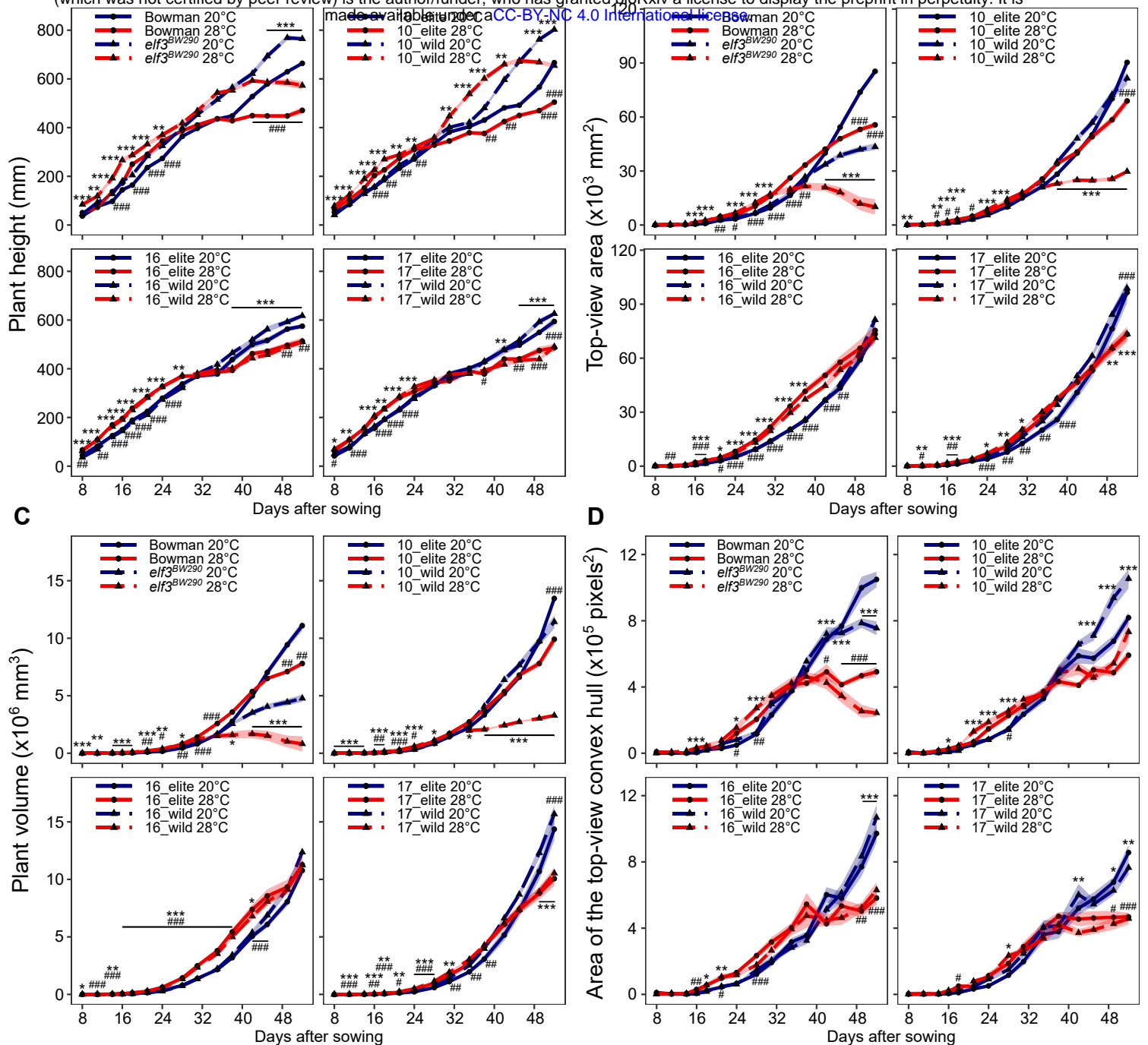


**Fig. 5.** Effects of exotic *ELF3* alleles and elevated temperatures on barley growth and plant architecture. (A-D) Bowman, *elf3<sup>BW290</sup>* and HIF pairs were grown in LD (16 h light/ 8 h dark) at day/night temperatures of 20/16°C (20°C). At 5 DAS, seedlings were shifted to 28/24°C (28°C) or were kept at 20°C. From 8 DAS, plants were imaged every two to four days. Plant height (A, average of two side-views) and top-view plant area (B) were obtained using HTPPheno pipeline. (C) Plant volume was estimated using plant area data from top-view (B) and two side-views. (D) Top-view convex hull area was obtained using Hull & Circle pipeline. Lines represent the mean and ribbons indicate SEM ( $n=11$ ). Hashtags (for Bowman and HIF elite lines with *HvELF3*) and asterisks (for *elf3<sup>BW290</sup>* and HIF wild lines with *HspELF3*) indicate significant differences between two temperature treatments (# and \*,  $P<0.05$ ; ## and \*\*,  $P<0.01$ ; ### and \*\*\*,  $P<0.001$ ; two-way ANOVA).

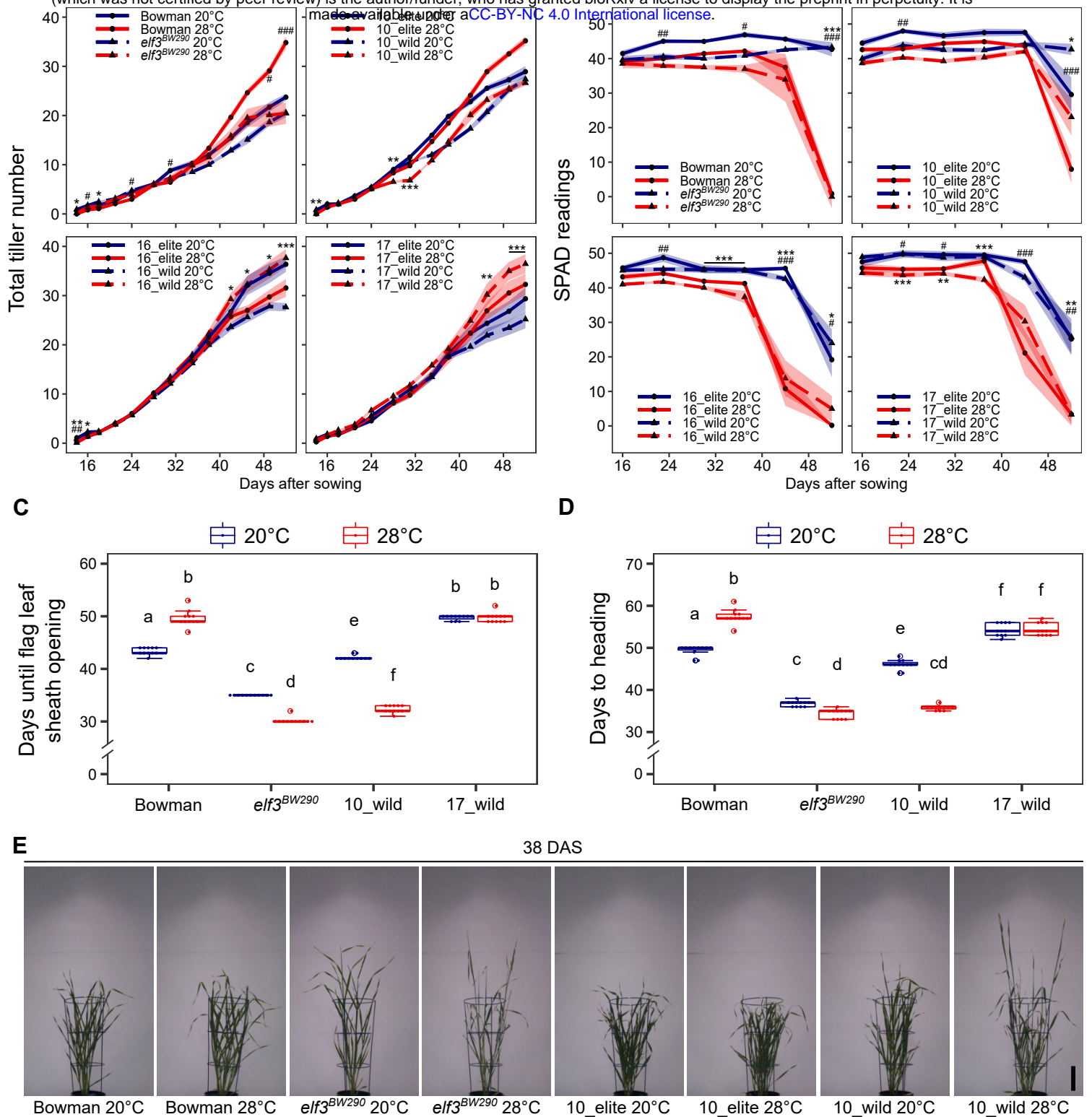


**Fig. 6.** Effects of exotic *ELF3* alleles and elevated temperatures on barley tillering, leaf senescence, and heading. (A-E) Bowman, *elf3<sup>BW290</sup>* and HIF pairs were grown in LD (16 h light/ 8 h dark) at day/night temperatures of 20/16°C (20°C). At 5 DAS, seedlings were shifted to 28/24°C (28°C) or were kept at 20°C. (A) Total tiller number was scored from 14 DAS. (B) Chlorophyll content of the second leaf was measured every week from 16 DAS. Lines represent the mean and ribbons indicate SEM ( $n=11$ ). Hashtags (for Bowman and HIF elite lines with *HvELF3*) and asterisks (for *elf3<sup>BW290</sup>* and HIF wild lines with *HspELF3*) indicate significant differences between two temperature treatments (# and \*,  $P<0.05$ ; ## and \*\*,  $P<0.01$ ; ### and \*\*\*,  $P<0.001$ ; two-way ANOVA). Days until flag leaf sheath opening (C) and heading (D) were scored in the lines showing visible awns before the end of the experiment. Boxes show medians and interquartile ranges. The whiskers extend to 1.5x interquartile ranges. Dots represent values of individual plants. Different letters above the boxes indicate significant differences (two-way ANOVA and Tukey's HSD test,  $P<0.05$ ). (E) Representative images of Bowman, *elf3<sup>BW290</sup>*, 10\_elite, and 10\_wild plants on 38 DAS. Scale bar = 10 cm.



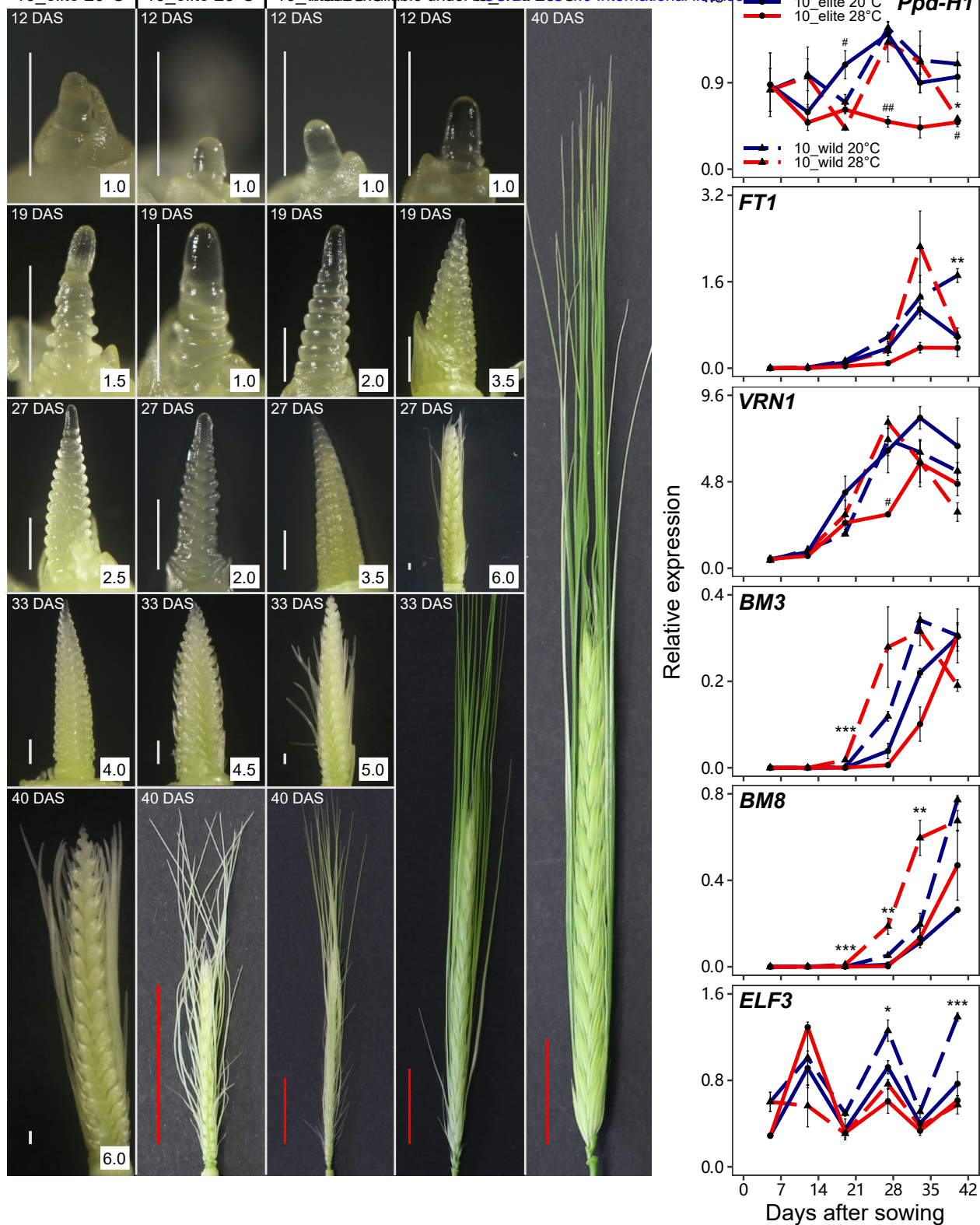


**Fig. 7.** An exotic *ELF3* allele interacts with elevated temperatures to control meristem development and the transcript levels of flowering genes. (A) Representative images of shoot apex meristem and inflorescence in 10\_elite and 10\_wild plants grown in LD (16 h light/ 8 h dark) at day/night temperatures of 20/16°C (20°C). At 5 DAS, seedlings were shifted to 28/24°C (28°C) or were kept at 20°C. Three plants were harvested per genotype per temperature at 12, 19, 27, 33, and 40 DAS. Figures in white boxes indicates Waddington scale scores until 6.0. Scale bars, white = 500 μm; red = 2 cm. (B) Transcript levels of barley flowering genes. Leaf samples were harvested at ZT08 during meristem dissection at each time point in (A), as well as at 5 DAS before the start of temperature treatment. Expression levels were normalized to *HvACTIN* and *HvGAPDH*. Error bars indicate the SEM ( $n=3$ ) of three biological replicates. Hashtags (for 10\_elite) and asterisks (for 10\_wild) indicate significant differences between two temperature treatments (# and \*,  $P<0.05$ ; ## and \*\*,  $P<0.01$ ; ### and \*\*\*,  $P<0.001$ ; two-way ANOVA).

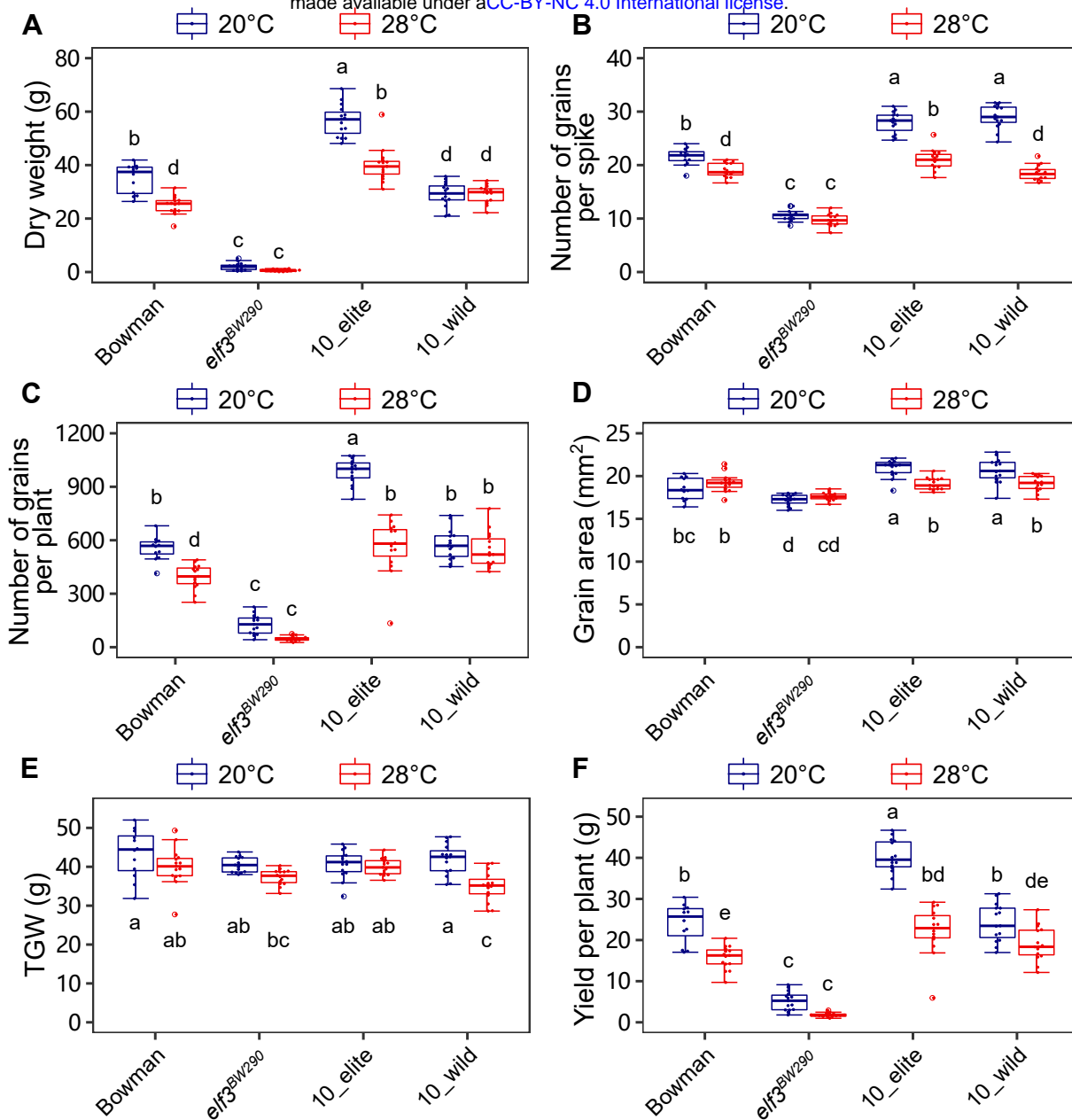


**Fig. 8.** An exotic *ELF3* allele mitigates yield loss at elevated temperatures. Bowman, *elf3<sup>BW290</sup>*, and HIF pair 10 plants were grown in greenhouse conditions with LD (16 h light/ 8 h dark) and day/night temperatures of 20/16°C (20°C). Plants reached three-leaf stage were shifted to 28/24°C (28°C) or were kept at 20°C. At maturity, plant dry weight (A), number of grains per spike (B) and per plant (C), grain area (D), thousand grain weight (E), and yield per plant (F) were scored. Boxes show medians and interquartile ranges. The whiskers extend to 1.5x interquartile ranges. Dots represent values of individual plants ( $n=12-15$ ). Different letters above or below the boxes indicate significant differences (two-way ANOVA and Tukey's HSD test,  $P<0.05$ ).

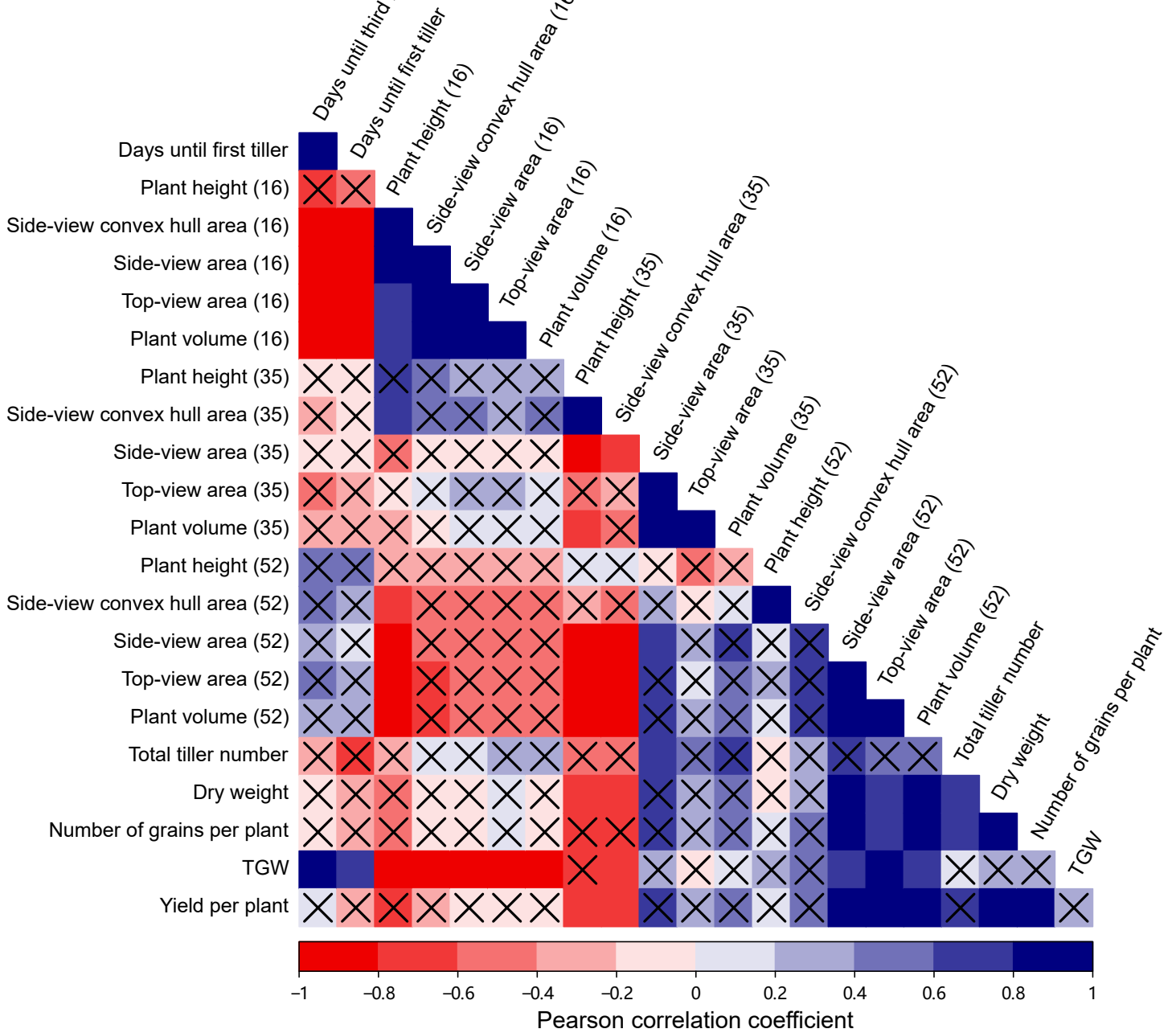


**Fig. 9.** Correlation of temperature responses in selected traits. Pairwise correlation coefficients were determined for Bowman, *elf3<sup>BW290</sup>*, and HIF pair 10 between selected traits obtained from both growth and development, and yield experiments. Numbers in the bracket indicate DAS. Pearson correlation coefficients were tested for significance and only significant coefficients with  $P < 0.05$  are not crossed. Correlations for all measured and derived growth curve modeling traits are shown in Supplementary Dataset S2.